RICE UNIVERSITY

LOW ENERGY ELASTIC AND FINE-STRUCTURE EXCITATION SCATTERING OF $C^+(^2P)$ BY $H(^2S)$

by

Jon Carleton Weisheit

A THESIS SUBMITTED
IN PARTIAL FULFILLMENT OF THE
REQUIREMENTS FOR THE DEGREE OF

DOCTOR OF PHILOSOPHY

Thesis Director's signature:

Houston, Texas

(July, 1970)

TABLE OF CONTENTS

I. INTRODUCTION

The interest in inelastic collisions between slow atoms has increased in recent years. Some general surveys[1,2] have emphasized the importance of such collisions in interstellar space and in the earth's atmosphere. In particular, calculations involving the collisions of H atoms with C, C^+, O, and Si^+ have shown the fine-structure excitation reactions to have rate coefficients large enough to provide significant cooling mechanisms for interstellar hydrogen clouds.[3-7] Also, the $O(^3P)$ - $O(^3P)$ reactions, of importance to the study of the earth's upper atmosphere, have been shown to have large excitation cross sections.[8]

The theoretical formulations presented in each of the investigations cited above assume that the collisions are elastic, or more precisely, that the energy differences among fine structure levels are negligible in comparison with the center-of-mass energy of motion of the colliding atoms. This approximation is usually introduced so that less computation is required to obtain scattering cross sections. We give in TABLE I-1 the excitation energies in degrees Kelvin [$T(^\circ K)$ = energy divided by Boltzmann's constant, k_B] for C, C^+, O, Si, and Si^+. If one considers the atomic collisions occurring in interstellar space, where the temperature is typically 100-200 °K, it is evident that the above-mentioned approximation is quite severe.

In this thesis we consider the scattering of singly ionized carbon

TABLE I-1. Excitation energies (°K) for the ground state fine-structure levels of C, C^+, O, Si and Si^+. The spectral data are from Reference 9.

Atom	Level	Excitation Energy (°K)
C	$^3P_0$	0
C	$^3P_1$	23
C	$^3P_2$	62
C^+	$^2P_{1/2}$	0
C^+	$^2P_{3/2}$	92
O	$^3P_2$	0
O	$^3P_1$	228
O	$^3P_0$	326
Si	$^3P_0$	0
Si	$^3P_1$	110
Si	$^3P_2$	321
Si^+	$^2P_{1/2}$	0
Si^+	$^2P_{3/2}$	411

by slow hydrogen atoms. The earlier calculations of Callaway and Dugan[6] and Smith[7] (who corrected the results given by Dalgarno and Rudge[3]) assume the C^+ - H excitation scattering to be elastic and then assume, respectively, that the collision is dominated by the long-range polarization interaction, and the spin-change interaction. Callaway and Dugan compute the excitation cross section using the impact parameter method[4], and Smith employs an orbiting approximation to the spin-change formalism for hyperfine transitions.[10] Herein, we consider both the long-range polarization interaction and the spin-change interaction (interpreted later as principally a short-range effect). The scattering problem is treated by a close-coupling formalism which does not neglect the energy difference between the $C^+(^2P)$ fine-structure levels. The long-range interaction is included in the coupled equations in a manner identical to that discussed by Arthurs and Dalgarno.[11] The spin-change interaction is included in a close coupling calculation - for the first time- by a somewhat novel modification of the elastic spin-change formalism.

The C^+ - H excitation cross section we compute varies from $174a_o^2$ at 0.01ev (116 °K) to $102a_o^2$ at 0.085ev(986 °K), and the maximum of almost $200a_o^2$ occurs near 0.015ev(174 °K). At all energies considered ($T < 1000$ °K) our excitation cross section is somewhat smaller than that reported by Smith but larger than that reported by Callaway and Dugan (see Figure 12).

Additional investigations indicate that most of the excitation cross section may be attributed to the spin-change interaction.

Studies of the sensitivity of our results to various input parameters and numerical methods suggest that the results reported in this thesis are accurate to $\pm$ 20 per cent.

The rest of the thesis is organized as follows. In Chapter II the close-coupling formalism for atom-atom collisions is developed, and the coupling matrix elements for the polarization and spin-change interactions evaluated. (These are derived in detail in the Appendices.) The numerical techniques used to integrate the coupled equations are described in Chapter III. In Chapter IV, the C^+ - H elastic and fine-structure excitation cross sections are presented and discussed, and the cooling rate due to this process calculated.

II. THEORY OF C^+ - H COLLISIONS AT LOW ENERGIES

A. General Atom-Atom Scattering Theory; Close Coupling Formalism

We begin our analysis of the interaction of two atoms with a discussion of the time-independent Schrodinger equation. In a coordinate system fixed in space we write the atom-atom Hamiltonian (atomic units are used throughout, i.e. $m_e = e = \hbar = 1$)

$$H = -\frac{1}{2M_a}\nabla_a^2 - \frac{1}{2M_b}\nabla_b^2 - \frac{1}{2}\sum_i \nabla_i^2 + V(\vec{R}_a, \vec{R}_b, \vec{r}_i), \quad (2.1)$$

where $\vec{R}_a$ and $\vec{R}_b$ locate the centers-of-mass of the nuclei of atoms A and B, M_a and M_b are the nuclear masses, V is the total interaction energy of the electrons and nuclei, and the summation is over all electrons. The unperturbed motion of the center-of-mass is not of interest here, so we procede to transform (2.1) to the relative and center-of-mass (CM) coordinates of the entire system.

If the number of electrons associated with atom A is n_a, and with B, n_b, the total mass is

$$M = M_a + M_b + n_a + n_b,$$

and the reduced mass of the two-atom system is

$$\mu = \left[(M_a + n_a)^{-1} + (M_b + n_b)^{-1} \right]^{-1}.$$

Let $\vec{R}$ be the vector joining the CM of atom A to that of atom B, and let $\vec{r}_{ai}$ designate the coordinates of electron (i) relative to the CM of nucleus A. The coordinates are illustrated in Figure 1. In terms of these coordinates the above Hamiltonian is

$$H = -\frac{1}{2M}\nabla_{CM}^2 - \frac{1}{2\mu}\nabla_R^2 - \frac{1}{2}\sum_{i=1}^{n_a}\nabla_{ai}^2 - \frac{1}{2}\sum_{j=1}^{n_b}\nabla_{bj}^2$$
$$- \frac{1}{2(M_a+n_a)}\sum_{(i,i')}\vec{\nabla}_{ai}\cdot\vec{\nabla}_{ai'} \qquad (2.2)$$
$$- \frac{1}{2(M_b+n_b)}\sum_{(j,j')}\vec{\nabla}_{bj}\cdot\vec{\nabla}_{bj'} + V(\vec{R},\vec{r}_{ai},\vec{r}_{bj}).$$

The notation $\sum_{(i,i')}$ indicates a summation over all pairs of electrons in a given atom. The mixed gradient terms in these summations are of order M_a^{-1} (M_b^{-1}) relative to the $\nabla_{ai}^2(\nabla_{bj}^2)$ terms. By dropping these terms we may separate the CM motion by writing the total wave function and energy as

$$\Psi_t = e^{i\vec{k}_{cm}\cdot\vec{R}_{cm}}\Phi, \qquad E_t = \frac{k_{cm}^2}{2M} + E,$$

where $\vec{k}_{cm}$ is the (constant) momentum of the center-of-mass, located at $\vec{R}_{cm}$, and E is the total energy less the kinetic energy of the CM. It follows that Φ, the function describing the relative and internal motion of the two atoms is a solution of the (approximate) wave equation

Figure 1. Coordinates for the atom-atom collision problem.

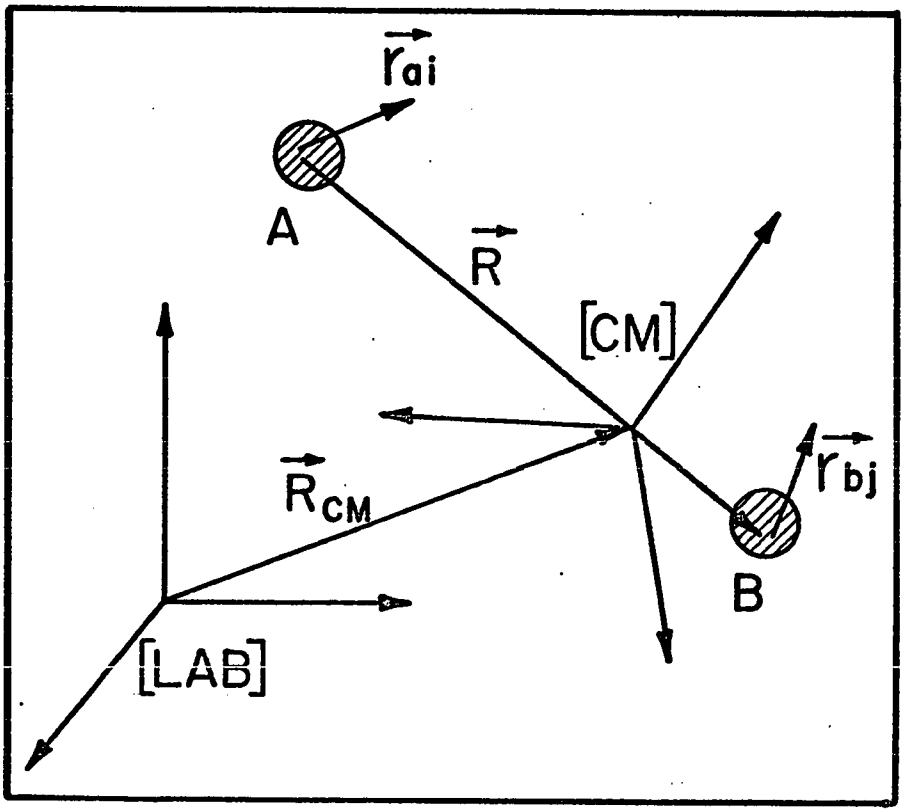
$\vec{r}_{ai}$
A
$\vec{R}$
[CM]
$\vec{R}_{CM}$
$\vec{r}_{bj}$
B
[LAB]

$$\left[-\frac{1}{2\mu}\nabla_R^2 - \frac{1}{2}\sum_i \nabla_{ai}^2 - \frac{1}{2}\sum_j \nabla_{bj}^2 + V(\vec{R},\vec{r}_{ai},\vec{r}_{bj}) - E\right]\Phi = 0. \tag{2.3}$$

In a manner analogous to the Born-Oppenheimer treatment of diatomic molecules[12] we seek solutions to (2.3) such that the relative motion may be considered separately. Let H(A) and H(B), $\phi_\alpha{}^A$ and $\phi_\beta{}^B$, and E^A and E^B be the Hamiltonians, antisymmetrized eigenfunctions, and eigenvalues for the separated atoms A and B, α and β being appropriate sets of quantum numbers. Then

$$H(A)\,\phi_\alpha^A = E_\alpha^A\,\phi_\alpha^A\,, \tag{2.4}$$

with a similar equation holding for atom B. Since the $\{\phi_\alpha{}^A\}$ and $\{\phi_\beta{}^B\}$ are complete sets we may expand the total wave function in terms of the product functions $\overline{\phi_\alpha{}^A\ \phi_\beta{}^B}$, the bar indicating antisymmetrization with respect to all electrons. Thus an incident plane wave may be written in terms of the functions

$$\Phi_{\alpha\beta}(\vec{R},\vec{r}_{ai},\vec{r}_{bj}) = F_{\alpha\beta}(\vec{R})\ \overline{\phi_\alpha^A(\vec{r}_{ai})\ \phi_\beta^B(\vec{r}_{bj})}\,. \tag{2.5}$$

Next we rewrite the Hamiltonian in (2.3) as

$$H = -\frac{1}{2\mu}\nabla_R^2 + H(A) + H(B) + V(\vec{R},\vec{r}_{ai},\vec{r}_{bj})\,, \tag{2.6}$$

with $\mathcal{V}$, the total interaction energy for the system, and make a partial wave expansion of $F_{\alpha\beta}$,

$$F_{\alpha\beta}(\vec{R}) = \frac{1}{R} \sum_{\ell m_\ell} f_{\alpha\beta}^{\ell m_\ell}(R)\, Y_{\ell m_\ell}(\hat{R}) . \tag{2.7}$$

$\hat{R}$ denotes the orientation of $\vec{R}$ in the CM system. Now using Equations (2.5) - (2.7) in (2.3) we find that the radial functions $f_{\alpha\beta}^{\ell m_\ell}(R)$ satisfy the following coupled equations:

$$\sum_{(\alpha\beta\ell m_\ell)} \Big[\frac{d^2}{dR^2} - \frac{\ell(\ell+1)}{R^2} - 2\mu \mathcal{V}(\vec{R},\vec{r}_{a_i},\vec{r}_{b_j}) + 2\mu\,(E - E_\alpha^A - E_\beta^B)\Big] \times f_{\alpha\beta}^{\ell m_\ell}(R)\, Y_{\ell m_\ell}(\hat{R})\, \overline{\phi_\alpha^A\, \phi_\beta^B} = 0 . \tag{2.8}$$

Premultiplying (2.8) by a particular $Y_{\ell m_\ell}^*(\hat{R})\, \overline{\phi_\alpha^A\, \phi_\beta^B}^*$ and integrating over all coordinates but R we obtain

$$\Big[\frac{d^2}{dR^2} - \frac{\ell(\ell+1)}{R^2} + k_{\alpha\beta}^2 \Big] f_{\alpha\beta}^{\ell m_\ell}(R) = 2\mu \sum_{(\alpha'\beta'\ell' m_\ell')} \langle \ell m_\ell\, \overline{\alpha\beta} \,|\, \mathcal{V} \,|\, \ell' m_\ell'\, \overline{\alpha'\beta'} \rangle\, f_{\alpha'\beta'}^{\ell' m_\ell'}(R) , \tag{2.9}$$

where

$$k_{\alpha\beta}^2 = 2\mu\,(E - E_\alpha^A - E_\beta^A) , \tag{2.10}$$

and the coupling matrix element

$$\langle l m_l \overline{\alpha\beta} \mid V \mid l' m_l' \overline{\alpha'\beta'} \rangle$$

$$= \int d\hat{R}\, d\vec{r}_{ai}\, d\vec{r}_{bj} \left[Y^*_{l m_l}(\hat{R})\, \overline{\phi^A_\alpha \phi^B_\beta}\, V\, Y_{l' m_l'}(\hat{R})\, \overline{\phi^A_{\alpha'} \phi^B_{\beta'}} \right]. \tag{2.11}$$

Formally, the scattering equations (2.9) may be simplified by expanding the wave function Ψ in a coupled representation. We first couple $\vec{j}_\alpha$, the total angular momentum of atom A, and $\vec{l}$, the angular momentum of relative motion, to yield $\vec{q}$, and then couple $\vec{q}$ and $\vec{j}_\beta$, the total angular momentum of atom B, to yield the total angular momentum $\vec{J}$. Then since the entire system is invariant with respect to spatial rotations, J^2 commutes with the total Hamiltonian (2.6) and, in fact, commutes with each term of this Hamiltonian. As a consequence the matrix elements (2.11) are diagonal in the coupled $|JM\rangle$ representation.

In this coupled representation we may expand the total wave function Ψ in terms of the functions

$$\Psi^{JM} = \sum_{(j_\alpha j_\beta l q)} \frac{1}{R}\, f^J_{j_\alpha j_\beta l q}(R)\, \Gamma^{JM}_{j_\alpha j_\beta l q}(\hat{R}, \vec{r}_{ai}, \vec{r}_{bj}), \tag{2.12}$$

where

$$\Gamma^{JM}_{j_\alpha j_\beta l g} = \sum_{m m_{j_\beta}} (g m\, j_\beta m_{j_\beta} \mid J M)\, \overline{\phi^{B}_{j_\beta m_{j_\beta}}(\vec{r}_{bj})\, \mathcal{Y}^{g m}_{j_\alpha l}(\hat{R}, \vec{r}_{ai})}\,, \tag{2.13}$$

$$\mathcal{Y}^{g m}_{j_\alpha l} = \sum_{m_l m_{j_\alpha}} (j_\alpha m_{j_\alpha} l m_l \mid g m)\, \phi^{A}_{j_\alpha m_{j_\alpha}}(\vec{r}_{ai})\, Y_{l m_l}(\hat{R})\,, \tag{2.14}$$

and $(j_1 m_1, j_2 m_2 \mid j m)$ is a Clebsch-Gordan coefficient.

Using (2.12), the scattering equations (2.9) become

$$\left[\frac{d^2}{dR^2} - \frac{l(l+1)}{R^2} + k^2_{\alpha\beta}\right] f^{J}_{j_\alpha j_\beta l g}(R) = 2\mu \sum_{(j'_\alpha j'_\beta l' g')} \langle \Gamma^{JM}_{j_\alpha j_\beta l g} \mid V \mid \Gamma^{JM}_{j'_\alpha j'_\beta l' g'} \rangle\, f^{J}_{j'_\alpha j'_\beta l' g'}(R)\,, \tag{2.15}$$

with

$$k^2_{\alpha\beta} = 2\mu\,(E - E^{A}_{j_\alpha} - E^{B}_{j_\beta})\,. \tag{2.16}$$

The analysis of scattering problems based upon the solution of the coupled equations (2.15) is usually referred to as the close coupling approximation. For brevity we shall indicate the initial state of the system by the set of quantum numbers,

$$\gamma_0 \Rightarrow \{j_{\alpha_0}\, j_{\beta_0}\, l_0\, g_0\, J\}\,,$$

and then write the radial functions for specified initial conditions as

$f_{\gamma\gamma_0}(R)$.

It is well-known[11,13] that the asymptotic forms of the radial functions $f_{\gamma\gamma_0}$ are related to elements of the unitary and symmetric scattering matrix S by

$$f_{\gamma\gamma_0} \underset{R\to\infty}{\sim} e^{-i(k_{\alpha\beta}R - l\pi/2)}\,\delta(\gamma,\gamma_0) - \left[\frac{k_0}{k_{\alpha\beta}}\right]^{1/2} e^{+i(k_{\alpha\beta}R - l\pi/2)}\,S(\gamma,\gamma_0). \quad (2.17)$$

Now defining the transition matrix

$$T = 1 - S, \quad (2.18)$$

the cross section for the $(\gamma_0 \to \gamma)$ transition is given by[11]

$$Q(\gamma,\gamma_0) = \frac{\pi}{\omega_0 k_0^2}\,|T(\gamma,\gamma_0)|^2, \quad (2.19)$$

where ω_0 is the statistical weight of the initial state.

In this paper we are concerned only with transitions between fine structure levels in one atom, say atom A, atom B not being altered by the collision. With the coupled representation described above, the cross section for the $(j_{\alpha_0} \to j_\alpha)$ transition may be written[11,14]

$$Q(j_\alpha, j_{\alpha_0}) = \frac{\pi}{k_0^2}\sum_{J=0}^{\infty}\frac{(2J+1)}{(2j_{\alpha_0}+1)(2j_{\beta_0}+1)}\sum_{(l_0 j_0)}|T(j_\alpha j_\beta l_0 j_0 J; j_{\alpha_0} j_{\beta_0} l_0 j_0 J)|^2. \quad (2.20)$$

In the next section we discuss in detail the interaction between C^+ and H, and evaluate the coupling matrix elements needed for the calculation of elastic and fine structure excitation scattering of $C^+(^2P)$ by $H(^2S)$.

B. C^+ - H Interaction; Evaluation of Coupling Matrix Elements

1. Long Range Interaction; Rotational Coupling Matrix Elements

At large values of the internuclear separation R the dominant forces between two atoms arise from electrostatic interactions. If the particles (i) in atom A have charges q_i and particles (j) in atom B, q_j, the electrostatic interaction energy is

$$\mathcal{V} = \sum_{i,j} \frac{q_i q_j}{|\vec{r}_{ai} - \vec{r}_{bj}|} = \sum_{i,j} \left(\frac{q_i q_j}{r_{ij}} \right) . \tag{2.21}$$

Specifically let $\vec{r}_{i1}$ be the vector from electron (i) on C^+ (atom A) to electron (1) on H (atom B), and define the vectors from the C^+ nuclear CM to electron (1) and from the H nuclear CM to electron (i) as $\vec{r}_{a1} = \vec{R} + \vec{r}_{b1}$ and $\vec{r}_{bi} = \vec{r}_{b1} - \vec{r}_{i1}$, respectively. Then the C^+ - H electrostatic interaction

$$\mathcal{V} = 6\left(\frac{1}{R} - \frac{1}{r_{a1}}\right) + \sum_{i=2}^{6} \left(\frac{1}{r_{i1}} - \frac{1}{r_{bi}} \right) . \tag{2.22}$$

To simplify the calculation of a coupling matrix element $\langle \Gamma^{JM}_{j_\alpha j_\beta l_j} | \times \mathcal{V} | \Gamma^{JM}_{j'_\alpha j'_\beta l' q'} \rangle$, we make the following approximation: at large separations R, where the C^+ - H interaction is dominated by the electrostatic term (2.22), the overlap of C^+ and H orbitals is small and consequently exchange terms may be neglected.[15] Then, since we do

not consider excitation of the C^+ core electrons, the integration over the spherical ($1s^2\ 2s^2$) C^+ orbitals may be performed easily, giving

$$\langle \Gamma^{JM}_{j_\alpha j_\beta \ell g} \mid v \mid \Gamma^{JM}_{j_\alpha' j_\beta' \ell' g'} \rangle \tag{2.23}$$

$$= \sum_{\left\{\begin{matrix} m m' \\ m_{j_\beta} m_{j_\beta}' \\ m_{j_\alpha} m_{j_\alpha}' \\ m_\ell m_\ell' \end{matrix}\right\}} \left(\begin{array}{l} (g m\, j_\beta m_{j_\beta} \mid J M)\ (g' m'\, j_\beta' m_{j_\beta'} \mid J M) \\ \times (j_\alpha m_{j_\alpha}\, \ell m_\ell \mid g m)\ (j_\alpha' m_{j_\alpha'}\, \ell' m_\ell' \mid g' m') \\ \times \langle \phi^{C^+}_{j_\alpha m_{j_\alpha}}(\vec{r}_{a2})\ \phi^{H}_{j_\beta m_{j_\beta}}(\vec{r}_{b1})\ Y_{\ell m_\ell}(\hat{R}) \mid \\ \times \tilde{v} \mid \phi^{C^+}_{j_\alpha' m_{j_\alpha'}}(\vec{r}_{a2})\ \phi^{H}_{j_\beta' m_{j_\beta'}}(\vec{r}_{b1})\ Y_{\ell' m_\ell'}(\hat{R}) \rangle \end{array} \right),$$

where

$$\tilde{v} = 2\left(\frac{1}{R} - \frac{1}{r_{a1}}\right) + \left(\frac{1}{r_{21}} - \frac{1}{r_{b2}}\right) \tag{2.24}$$

is just the electrostatic interaction of the $C^+(1s^2\ 2s^2)$ core, charge +2 and the C^+ valence electron with the hydrogen atom.

Now the full solution of the scattering equations (2.15) requires the evaluation of an infinite number of the integrals (2.23). To make the problem tractable it is common to restrict the product functions (2.5) to some finite number of atomic states, $\phi^{C^+}_\alpha$ and ϕ^{H}_β. If we retain only those states that are energetically accessible ($k^2_{\alpha\beta} \geq 0$), i.e. keep only "open" channels, we see that for energies considered herein we need just the states arising from the ground configurations $C^+(^2P)$ and $H(^2S)$.

However, the interaction $\tilde{\mathcal{V}}$ averaged with respect to the spherical H(1s) orbital (the first order energy correction for the H atom) vanishes;[9] thus there is no long-range first order electrostatic interaction energy between C^+ and H if exchange is neglected.

For transitions between the fine-structure levels of $C^+(^2P)$ to result from the electrostatic interaction (2.24), if we neglect exchange evidently we must consider closed channels. We choose to include the entire spectrum of hydrogen states $\{\phi_\beta^H\}$ but only the $C^+(^2P)$ states in the expansion of the total wave function. This selection is now shown to be consistent with the C^+ - H collision being viewed as a carbon ion being scattered by the potential field of a polarized hydrogen atom.[6]

Using the Hamiltonian (2.6) with $\tilde{\mathcal{V}}$ instead of $\mathcal{V}$, neglecting exchange we obtain from the Schrodinger equation

$$\sum_{\alpha\beta} (\nabla_{\vec{R}}^2 + k_{\alpha\beta}^2) F_{\alpha\beta}(\vec{R})\, \phi_\alpha^{C^+} \phi_\beta^H = 2\mu \sum_{\alpha\beta} \tilde{\mathcal{V}}(\vec{R}, \vec{r}_{a1}, \vec{r}_{b1})\, F_{\alpha\beta}(\vec{R})\, \phi_\alpha^{C^+} \phi_\beta^H \tag{2.25}$$

where the summations are over all hydrogen states and all $C^+(^2P)$ states. Multiplying (2.25) by ϕ_0^{H*}, the ground state hydrogen wave function, and integrating with respect to $\vec{r}_{b1}$,

$$\sum_\alpha (\nabla_R^2 + k_{\alpha 0}^2) F_{\alpha 0}(\vec{R})\, \phi_\alpha^{C^+} = 2\mu \sum_{\alpha\beta} \tilde{\mathcal{V}}_{0\beta} F_{\alpha\beta}(\vec{R})\, \phi_\alpha^{C^+} \,, \tag{2.26}$$

where

$$\tilde{\mathcal{V}}_{o\beta}(\vec{R},\vec{r}_{a2}) = \int d\vec{r}_{b1}\left[\phi_o^{H*}(\vec{r}_{b1})\,\tilde{\mathcal{V}}(\vec{R},\vec{r}_{a2},\vec{r}_{b1})\,\phi_\beta^{H}(\vec{r}_{b1})\right] \quad (2.27)$$

We noted earlier that $\tilde{\mathcal{V}}_{oo}$ vanishes so that, for $k_{\alpha\beta}^2 < 0$ when $\beta \neq 0$, the sum on the right hand side of (2.26) includes only closed channels. Following the argument of Castillejo, et. al,[16] it may be shown that the quantity

$$\sum_{\beta\neq 0} \tilde{\mathcal{V}}_{o\beta}\, F_{\alpha\beta}(\vec{R})$$

behaves asymptotically as

$$\sum_{\beta\neq 0} \tilde{\mathcal{V}}_{o\beta}\, F_{\alpha\beta}(\vec{R}) \underset{R\to\infty}{\sim} \left\{ \sum_{\beta\neq 0} \frac{|\tilde{\mathcal{V}}_{o\beta}|^2}{(E_o^H - E_\beta^H)} \right\} F_{\alpha o}(\vec{R}) \,. \quad (2.28)$$

The bracketed term in (2.28) is readily identified as the second order energy correction W for a ground state hydrogen atom perturbed by the potential $\tilde{\mathcal{V}}$.

Returning to (2.26), if we substitute the result (2.28), multiplying by a particular ϕ_α^{c+*} and integrating with respect to the coordinates $\vec{r}_{a2}$ we find

$$\left(\nabla_R^2 + k_{\alpha o}^2\right) F_{\alpha o}(\vec{R}) = 2\mu \sum_{\alpha'} \langle \alpha | W(\vec{R},\vec{r}_{a2}) | \alpha' \rangle F_{\alpha' o}(\vec{R}) \,. \quad (2.29)$$

With the expansion of $F(\vec{R})$ given by (2.7), in the representation described by (2.12) - (2.14), Equation (2.29) reduces to

$$\left[\frac{d^2}{dR^2} - \frac{l(l+1)}{R^2} + k_j^2\right] f^J_{jlj,j_0l_0j_0}(R)$$

$$= 2\mu \sum_{(j'l'j'm')} \langle Y^{jm}_{jl} | W | Y^{j'm'}_{j'l'} \rangle f^J_{j'l'j',j_0l_0j_0}(R) \,, \tag{2.30}$$

where $\vec{j}$ is the total angular momentum of the carbon ion. The coupled equations (2.30) describe the scattering of C^+ by an orientation-dependent potential $W(\vec{R},\vec{r}_{a2})$ produced by the polarized hydrogen atom, and they have the same form as those discussed by Arthurs and Dalgarno[11], and Lane and Geltman.[14]

The details of the calculation of W are presented in Appendix A; therein we show that through terms of the order R^{-6},

$$W(\vec{R},\vec{r}) = -\frac{\alpha_2}{2R^4}\left\{1 - 4\frac{r}{R}P_1(\vec{R}\cdot\vec{r}) + \left(\frac{r}{R}\right)^2\left[2 - 4P_2(\vec{R}\cdot\vec{r})\right]\right\} - \frac{\alpha_4}{2R^6} + \mathcal{O}(R^{-7}) \,, \tag{2.31}$$

where α_{2L} is the 2^L-pole polarizability of hydrogen, $\vec{r}$ denotes the coordinates of the $C^+(2p)$ electron, and $P_\lambda(\vec{R}\cdot\vec{r})$ is the λ th order Legendre polynomial whose argument is the cosine of the angle between $\vec{R}$ and $\vec{r}$. Except for the additional term $-\frac{\alpha_4}{2R^6}$ the above

expression is identical to that used by Callaway and Dugan.

Employing the spherical harmonic addition theorem,

$$P_\lambda(\vec{R}\cdot\vec{r}) = \left(\frac{2\lambda+1}{4\pi}\right) \sum_\mu Y^*_{\lambda\mu}(\hat{R})\, Y_{\lambda\mu}(\hat{r}) \,, \tag{2.32}$$

we can rewrite the interaction W in the general form

$$W(\vec{R},\vec{r}) = \sum_{\lambda\mu} W_\lambda(R,r) \left(\frac{2\lambda+1}{4\pi}\right) Y^*_{\lambda\mu}(\hat{R})\, Y_{\lambda\mu}(\hat{r}) \,. \tag{2.33}$$

Then the coupling matrix elements in (2.30) may be reduced by Racah algebra techniques[11] to give

$$\begin{aligned}
&\langle \mathcal{Y}^{jm}_{jl} | W | \mathcal{Y}^{j'm'}_{j'l'} \rangle \\
&= 3\,\delta(q,q')\,\delta(m,m')\left[(2l+1)(2l'+1)(2j+1)(2j'+1)\right]^{1/2} \\
&\quad \times \sum_\lambda (-)^{j-1/2-\lambda} W_\lambda(R) \begin{pmatrix} l & \lambda & l' \\ 0 & 0 & 0 \end{pmatrix} \begin{pmatrix} l & \lambda & l' \\ 0 & 0 & 0 \end{pmatrix} \qquad (2.34) \\
&\quad \times \begin{Bmatrix} j & j' & \lambda \\ 1 & 1 & 1/2 \end{Bmatrix} \begin{Bmatrix} j & j' & \lambda \\ l' & l & j \end{Bmatrix} \\
&= \sum_\lambda W_\lambda(R)\, q_\lambda(jlj, j'l'j') \,, \text{ say,}
\end{aligned}$$

where $\begin{pmatrix} j_1 & j_2 & j_3 \\ m_1 & m_2 & m_3 \end{pmatrix}$ is a 3-j symbol,[17] $\begin{Bmatrix} j_1 & j_2 & j_3 \\ j_4 & j_5 & j_6 \end{Bmatrix}$ is a 6-j symbol,[17] and the W_λ have now been averaged with respect to the $C^+(2p)$ orbital. The details of this reduction are given in Appendix B.

Now, the utility of our particular coupling scheme is apparent: the coupling matrix elements q_λ are diagonal in j and M and independent of M, and also independent of J.

It is obvious from the terms appearing in q_λ that at large nuclear separations changes in the internal angular momentum j of C^+ are possible because j is coupled to the rotational angular momentum of relative motion l by the non-spherical part of the interaction potential. (Note that $q_0(jlj,j'l'j') = \delta(j,j')\delta(l,l')\delta(j,j')$.) Subsequently, then, we shall refer to this situation as rotational coupling.

In Part 2 we discuss the spin-change coupling mechanism which is of particular importance at small nuclear separations and in Section C we modify the scattering equations (2.30) to include this effect.

2. Short-Range Interaction; Spin-Change Coupling Matrix Elements

In a spin-change collision the internal angular momenta of colliding systems change as a result of the exchange of electrons with different spin orientations. This process is important only when the internuclear separation is small enough to allow significant overlap of the atomic orbitals. The quantal formulation of a spin-change process has been given by Dalgarno[10] and applied by several authors[3,5,7,18,19] to the study of various atom-atom interactions.

As presented by Dalgarno this process is elastic. We now review the essential concepts of his formulation. In terms of initial product atomic states $\overline{\psi^A_{j_\alpha m_{j\alpha}} \psi^B_{j_\beta m_{j\beta}}}$ quantized along $\vec{R}$, the total wave function for the colliding atoms has the asymptotic form

$$\Psi(j_\alpha m_{j\alpha} j_\beta m_{j\beta}) \underset{R\to\infty}{\sim} e^{i\vec{k}\cdot\vec{R}} \overline{\psi^A_{j_\alpha m_{j\alpha}} \psi^B_{j_\beta m_{j\beta}}} + \frac{1}{R} e^{ikR} \sum_{(j'_\alpha m'_{j\alpha} j'_\beta m'_{j\beta})} \overline{\psi^A_{j'_\alpha m'_{j\alpha}} \psi^B_{j'_\beta m'_{j\beta}}} f(j'_\alpha m'_{j\alpha} j'_\beta m'_{j\beta}, j_\alpha m_{j\alpha} j_\beta m_{j\beta}; \hat{R}), \tag{2.35}$$

where, as before, $\hat{R}$ denotes the angles between $\vec{R}$ and $\vec{k}$ and the bar denotes antisymmetrization with respect to all electrons.

Now let the quantum numbers Λ, S, and M_S describe a stationary state χ of the molecule AB, and represent the total projected (onto $\vec{R}$) orbital angular momentum, the total spin angular momentum,

and its projection (onto $\vec{R}$), respectively. Then if spin-orbit and spin-spin interactions in the molecule are neglected, in this representation[5,18] the total wave function behaves asymptotically as

$$\Psi(j_\alpha m_{j_\alpha} j_\beta m_{j_\beta}) \underset{R\to\infty}{\sim} \sum_{\Lambda S M_S} \langle j_\alpha m_{j_\alpha} j_\beta m_{j_\beta} | \Lambda S M_S \rangle \chi_{\Lambda S M_S} \times \left[e^{i\vec{k}\cdot\vec{R}} + \frac{1}{R} e^{ikR} f(\Lambda S M_S, \Lambda S M_S; \hat{R}) \right] \tag{2.36}$$

where $\langle j_\alpha m_{j_\alpha} j_\beta m_{j_\beta} | \Lambda S M_S \rangle$ is a coupling coefficient.

Equating (2.35) and (2.36) it can be shown that the scattering amplitude for the transition $\{j_\alpha m_{j_\alpha} j_\beta m_{j_\beta}\} \Rightarrow \{j'_\alpha m'_{j_\alpha} j'_\beta m'_{j_\beta}\}$ is given by

$$f(j'_\alpha m'_{j_\alpha} j'_\beta m'_{j_\beta}, j_\alpha m_{j_\alpha} j_\beta m_{j_\beta}; \hat{R}) = \sum_{\Lambda S M_S} \langle j'_\alpha m'_{j_\alpha} j'_\beta m'_{j_\beta} | \Lambda S M_S \rangle f(\Lambda S M_S, \Lambda S M_S; \hat{R}) \langle \Lambda S M_S | j_\alpha m_{j_\alpha} j_\beta m_{j_\beta} \rangle . \tag{2.37}$$

Equation (2.37) provides a simple physical interpretation of the spin-change process: the atoms initially in states $(j_\alpha m_{j_\alpha})$ and $(j_\beta m_{j_\beta})$ approach each other with their angular momenta coupling to form a particular molecular stationary state $\chi_{\Lambda S M_S}$; then after scattering elastically, the atoms separate and the (same) molecular state is "uncoupled," yielding final atomic states $(j'_\alpha m'_{j_\alpha})$ and $(j'_\beta m'_{j_\beta})$. We emphasize that we do not use Equation (2.37). It has been given

only to illustrate the nature of the spin-change process.

To incorporate the concept of the spin-change interaction in the close coupling formalism developed in Section A, we begin with the coupled equations (2.15). Including only the terms arising from the ground state configurations $C^+(^2P)$ and $H(^2S)$, we may drop the constant total angular momentum $j_\beta = 1/2$ of the hydrogen atom from the notation and write

$$\left[\frac{d^2}{dR^2} - \frac{l(l+1)}{R^2} + k_j^2\right] f^J_{jlj,\, j_0 l_0 j_0}(R)$$

$$= 2\mu \sum_{j'l'j'} \langle \Gamma^{JM}_{jlj} \,|\, V \,|\, \Gamma^{JM}_{j'l'j'} \rangle \, f^J_{j'l'j',\, j_0 l_0 j_0}(R) \,, \tag{2.38}$$

where the coupling matrix element

$$\langle \Gamma^{JM}_{jlj} \,|\, V \,|\, \Gamma^{JM}_{j'l'j'} \rangle$$

$$= \sum_{\substack{mm' \\ m_j m_j' \\ m_l m_l' \\ \sigma\sigma'}} \left(\begin{array}{l} (j m_j l m_l \,|\, j m)(j m \tfrac{1}{2} \sigma \,|\, J M) \\ \times (j' m_j' l' m_l' \,|\, j' m')(j' m' \tfrac{1}{2} \sigma' \,|\, J M) \\ \times \langle Y_{l m_l}(\hat{R})\, \overline{\phi^{C^+}_{j m_j}\, \phi^{H}_{\frac{1}{2}\sigma}} \,|\, V \,|\, Y_{l' m_l'}(\hat{R})\, \phi^{C^+}_{j' m_j'}\, \phi^{H}_{\frac{1}{2}\sigma'} \rangle \end{array} \right) . \tag{2.39}$$

The antisymmetrized atomic wave functions in (2.39) are quantized with respect to the CM coordinate system. These wave functions are related to the wave functions $\overline{\Psi^{c+}_{jm}\ \Psi^{H}_{1/2\sigma}}$ quantized with respect to the body axis $\vec{R}$ by

$$\overline{\phi^{c+}_{jm}\,\phi^{H}_{1/2\sigma}} = \sum_{\tilde{m}_j\tilde{\sigma}} D^{j}_{\tilde{m}_j m_j}(\varphi_R,\vartheta_R,0)\, D^{1/2}_{\tilde{\sigma}\sigma}(\varphi_R,\vartheta_R,0)\ \overline{\Psi^{c+}_{j\tilde{m}_j}\ \Psi^{H}_{1/2\tilde{\sigma}}} \tag{2.40}$$

$$= \sum_{\tilde{m}_j\tilde{\sigma}} D^{j}_{\tilde{m}_j m_j}(\hat{R})\, D^{1/2}_{\tilde{\sigma}\sigma}(\hat{R})\ \overline{\Psi^{c+}_{j\tilde{m}_j}\ \Psi^{H}_{1/2\tilde{\sigma}}}\ .$$

The coefficients D are elements of the rotation matrices, discussed at length by Rose.[20]

Further, the wave functions $\overline{\Psi^{c+}_{jm_j}\ \Psi^{H}_{1/2\sigma}}$ may be related to stationary states of the CH^+ molecule $\chi_{\Lambda S M_s}$ at large nuclear separations R by a straight foreward recoupling of angular momenta,

$$\chi_{\Lambda S M_s} \underset{R\to\infty}{\sim} \sum_{jm_j\sigma} \overline{\Psi^{c+}_{jm_j}\ \Psi^{H}_{1/2\sigma}}\ \langle j m_j \sigma\,|\,\Lambda S M_s\rangle\ , \tag{2.41}$$

where the coupling coefficient

$$\langle j m_j \sigma\,|\,\Lambda S M_s\rangle$$

$$= (1\,m\,0\,0\,|\,1\,\Lambda)(1\,m\,1/2\,m_s\,|\,j\,m_j)(1/2\,m_s\,1/2\,\sigma\,|\,S M_s)\ . \tag{2.42}$$

For the sake of simplicity we now assume that the recoupling

transformation is valid at all nuclear separations.

If we neglect spin-orbit and spin-spin interactions - in keeping with the spin-change formalism discussed above - we observe that $\mathcal{N}$ is diagonal in the $(\Lambda S M_S)$ representation, and that, for a specific Λ and S, the diagonal matrix element $\langle \chi_{\Lambda S M_s} | \mathcal{N} | \chi_{\Lambda S M_s} \rangle$ is independent of M_S. Further, neglecting at this point the $C^+(^2P)$ fine-structure energy defect, we may approximate the matrix element

$$\mathcal{N}_{\Lambda S}(R) \equiv \langle \chi_{\Lambda S M_s} | \mathcal{N} | \chi_{\Lambda S M_s} \rangle$$

$$= E_{\Lambda S}(R) + \frac{q_A q_B}{R} - \langle \chi_{\Lambda S M_s} | H(C^+) + H(H) | \chi_{\Lambda S M_s} \rangle \quad (2.43a)$$

$$\simeq E_{\Lambda S}(R) + \frac{q_A q_B}{R} - \left(E_j^{C^+} + E_{1/2}^{H} \right), \quad (2.43b)$$

where $E_{\Lambda S}(R)$ is the electronic energy of the molecular state $\chi_{\Lambda S}$ and q is the nuclear charge. Equation (2.43b) is correct asymptotically (for a given $C^+(^2P_j)$ level), and should be reasonably accurate at small nuclear separations since the quantity $\langle \chi_{\Lambda S M_s} | H(C^+) + H(H) | \chi_{\Lambda S M_s} \rangle$ is not strongly R-dependent. For simplicity we use $E_{j=1/2}^{C^+}$ throughout, and allow for the energy defect by using the correct k^2 in the scattering equations (2.38). This scheme does of course affect the accuracy of our calculations when $k_0^2 \gtrsim \Delta k^2$, but we may anticipate our results and note that the approximation $\Delta k^2 = 0$ is not very severe even at low energies.

Upon combining the results (2.40), (2.41), and (2.43) it follows that the coupling matrix element

$$
\begin{aligned}
&\langle \Gamma^{JM}_{j\ell g} \,|\, V \,|\, \Gamma^{JM}_{j'\ell'g'} \rangle \\
&= \sum V_{\Lambda S}(R)\ (j m_j \ell m_\ell \,|\, g m)(g m \tfrac{1}{2}\sigma \,|\, J M) \\
&\qquad \times (j' m_j' \ell' m_\ell' \,|\, g' m')(g' m' \tfrac{1}{2}\sigma' \,|\, J M) \qquad (2.44) \\
&\qquad \times \langle j \tilde{m}_j \tilde{\sigma} \,|\, \Lambda S M_S \rangle \langle \Lambda S M_S \,|\, j' \tilde{m}_j' \tilde{\sigma}' \rangle \\
&\qquad \times \langle Y_{\ell m_\ell}\ D^{j}_{\tilde{m}_j m_j}\ D^{1/2}_{\tilde{\sigma}\sigma} \,|\, Y_{\ell' m_\ell'}\ D^{j'}_{\tilde{m}_j' m_j'}\ D^{1/2}_{\tilde{\sigma}'\sigma'} \rangle \ .
\end{aligned}
$$

In Appendix C we show that this expression can be reduced by Racah algebra techniques to yield

$$
\langle \Gamma^{JM}_{j\ell g} \,|\, V \,|\, \Gamma^{JM}_{j'\ell'g'} \rangle = \sum_{\Lambda S} P^{J}_{\Lambda S}(j\ell g; j'\ell' g')\, V_{\Lambda S}(R)\ , \qquad (2.45)
$$

where the coupling coefficient

$$
\begin{aligned}
&P^{J}_{\Lambda S}(j\ell g, j'\ell' g') \\
&= (2S+1)\left[(2j+1)(2j'+1)(2\ell+1)(2\ell'+1)(2g+1)(2g'+1)\right]^{1/2} \\
&\quad \times (-)^{1-J-S-g-g'} \sum_{abc} (2a+1)(2b+1) \begin{pmatrix} \ell & \ell' & c \\ 0 & 0 & 0 \end{pmatrix} \qquad (2.46) \\
&\quad \times \begin{Bmatrix} J & \ell & a \\ j & \tfrac{1}{2} & g \end{Bmatrix} \begin{Bmatrix} J & \ell' & b \\ j' & \tfrac{1}{2} & g' \end{Bmatrix} \begin{Bmatrix} 1 & a & S \\ \tfrac{1}{2} & \tfrac{1}{2} & j \end{Bmatrix} \begin{Bmatrix} 1 & b & S \\ \tfrac{1}{2} & \tfrac{1}{2} & j' \end{Bmatrix} \\
&\quad \times \begin{Bmatrix} \ell' & \ell & c \\ 0 & 0 & 0 \end{Bmatrix} \begin{Bmatrix} 1 & 1 & c \\ a & b & S \end{Bmatrix} \sum_{|m|=\Lambda} (-)^{m} \begin{pmatrix} 1 & 1 & c \\ -m & m & 0 \end{pmatrix} .
\end{aligned}
$$

Because here S = 0 or 1, the summations indices (a, b, c) are restricted to the values 0, 1, and 2.

Upon substituting (2.45) into (2.38) we find

$$\left[\frac{d^2}{dR^2} - \frac{\ell(\ell+1)}{R^2} + k_j^2\right] f^J_{j\ell g, j_0 \ell_0 g_0}(R)$$

$$= 2\mu \sum_{\Lambda S} v_{\Lambda S}(R) \sum_{j'\ell' g'} P^J_{\Lambda S}(j\ell g, j'\ell' g') \, f^J_{j'\ell' g', j_0 \ell_0 g_0}(R) \, . \tag{2.47}$$

We may interpret the coupling terms on the RHS of (2.47) as providing an extension of the long-range coupling matrix elements

$W_\lambda(R)\, q_\lambda(j\ell g, j'\ell' g')$ to small nuclear separations. Moreover, these coupling terms provide for the possibility of exchange in each molecular state (ΛS) through the angular momentum recoupling formalism characteristic of spin-change processes.

In the next section we give a prescription for modifying the scattering equations (2.30), valid at large nuclear separations, so that at small R-values the equations take the form (2.47).

C. The C^+ - H Scattering Equations

To incorporate the spin-change coupling mechanism in the scattering equations (2.30), we take advantage of the fact that all $V_{\Lambda S}(R)$ tend asymptotically to the value $W_0(R)$, the dominant term of the long-range interaction. Thus, from (2.45),

$$\langle \Gamma^{JM}_{jlg} | V | \Gamma^{JM}_{j'l'g'} \rangle \underset{R\to\infty}{\sim} W_0(R) \sum_{\Lambda S} P^J_{\Lambda S}(jlg, j'l'g'). \qquad (2.48)$$

The summation over Λ and S may be performed by noting that the quantity

$$\sum_{\Lambda} \sum_{|m|=\Lambda} (-)^m \begin{pmatrix} 1 & 1 & c \\ -m & m & 0 \end{pmatrix} = \sum_{m} (-)^m \begin{pmatrix} 1 & 1 & c \\ -m & m & 0 \end{pmatrix} = -\sqrt{3}\,\delta(c,0) \qquad (2.49)$$

vanishes unless $c = 0$ [17]. Then using the relationships

$$\begin{Bmatrix} j_1 & j_2 & 0 \\ j_3 & j_4 & j_5 \end{Bmatrix} = \frac{\delta(j_1,j_2)\,\delta(j_3,j_4)\,(-)^{j_1+j_3+j_5}}{[(2j_1+1)(2j_3+1)]^{1/2}}, \qquad (2.50)$$

and

$$\sum_{x} (2x+1) \begin{Bmatrix} j_1 & j_2 & x \\ j_3 & j_4 & j_5 \end{Bmatrix} \begin{Bmatrix} j_3 & j_4 & x \\ j_1 & j_2 & j_6 \end{Bmatrix} = \frac{\delta(j_5,j_6)}{(2j_5+1)}, \qquad (2.51)$$

summing over S and then a we obtain

$$\sum_{\Lambda S} P^{J}_{\Lambda S}(jlq, j'l'q') = \delta(j,j')\delta(l,l')\delta(q,q'). \quad (2.52)$$

Consequently, as the differences between the molecular curves $U_{\Lambda S}(R)$ vanish, the coupling matrix elements

$$\langle \Gamma^{JM}_{jlq} | U | \Gamma^{JM}_{j'l'q'} \rangle \underset{R\to\infty}{\sim} W_0(R)\,\delta(j,j')\delta(l,l')\delta(q,q') \quad (2.53)$$
$$= W_0(R)\, q_0(jlq, j'l'q').$$

Our prescription for including both spin-change and rotational coupling in the C^+ - H scattering equations is as follows: at some intermediate value $R = R_m$ where $W_2 \ll W_0$ and where all $U_{\Lambda S} \approx W_0$ we match the $U_{\Lambda S}$ and W_0, requiring

$$U_{\Lambda S}(R) \equiv W_0(R), \text{ for all } R \geq R_m. \quad (2.54)$$

For $R \geq R_m$ there is no spin-change coupling. For $R < R_m$, $W_2(R)$ is rapidly cut off since, in this inner region, the "effective" W_2 is contained in the $U_{\Lambda S}(R)$. By explicitly retaining the (small) W_2 term beyond R_m we allow for rotational coupling at large nuclear separations. The scattering equations now take the form

$$\left[\frac{d^2}{dR^2} - \frac{l(l+1)}{R^2} + k_j^2\right] f^J_{jlg,\, j_0 l_0 g_0}(R)$$

$$= 2\mu \sum_{j'l'g'} \left\{\left[\sum_{\Lambda S} P^J_{\Lambda S}(jlg, j'l'g')\, V_{\Lambda S}(R)\right]\right. \tag{2.55}$$

$$\left. + \tilde{W}_2(R)\, q_2(jlg, j'l'g')\right\} f^J_{j'l'g',\, j_0 l_0 g_0}(R)\,,$$

where $\tilde{W}_2(R)$ indicates that $W_2(R)$ is modified as indicated above.

Inspection of the coupling terms in (2.55) reveals that, for each of the total angular momentum J, there are 12 coupled differential equations. Fortunately, each set of 12 separates into two sets of 6 coupled equations, one containing channels with only even partial waves l, the other, only odd partial waves. These will subsequently be referred to as even and odd parity channels, respectively.

In Chapter III we describe the numerical methods used to solve the coupled equations (2.55) on high speed computers. The CH^+ curves $V_{\Lambda S}(R)$ used in our calculations are also discussed.

III. NUMERICAL TECHNIQUES

A. C^+ - H Potential Energy Curves

To determine the spin-change contribution to the cross sections for $C^+(^2P)$ and $H(^2S)$ collisions, detailed knowledge of the potential energy curves for CH^+ states arising from the ground configurations of the separated atoms is required.

For the $^3\Sigma^+$ and $^3\Pi$ curves, we have used values given by Moore;[21] for the $^1\Sigma^+$ and $^1\Pi$ curves, the more recent calculations of Browne[22] were used. All of these data are given in TABLE III-1. Briefly, their calculations were made as follows,

$^3\Sigma^+$: 5 term expansion of Slater-type orbitals, with optimization of some orbital exponents.

$^3\Pi$: 5 term expansion of Slater-type orbitals, with no optimization of orbital exponents.

$^1\Sigma^+$: 19 term expansion of Slater-type orbitals with optimization of some orbital exponents.

$^1\Pi$: 15 term expansion of Slater-type orbitals, with the orbital exponents optimized at each R-value.

Additional details may be obtained from the research reported by Moore, Browne, and Matsen.[23]

For our purposes, each of the four curves is appropriately increased or decreased a constant amount for all R so that asymptotically the curves yield the energy of the separated $C^+(^2P)$ and $H(^2S)$

TABLE III-1. The CH^+ potential energy curves $^3\Sigma^+$, $^3\Pi$, $^1\Sigma^+$, and $^1\Pi$. The data are from References 21 and 22.

R(a_o)	$^3\Sigma^+$(a.u.)	$^3\Pi$(a.u.)	$^1\Sigma^+$(a.u.)	$^1\Pi$(a.u.)
1.0			-37.046	-36.907
1.5			-37.767	-37.612
1.7			-37.855	-37.701
1.9	-37.284	-37.793	-37.898	-37.474
2.0	-37.337			
2.1		-37.815		
2.2	-37.427		-37.916	-37.778
2.3		-37.821	-37.916	-37.782
2.4	-37.499		-37.913	-37.785
2.5		-37.819	-37.909	-37.785
2.7	-37.580			
2.8			-37.891	-37.785
3.0	-37.636	-37.805	-37.878	-37.782
3.5	-37.692		-37.846	-37.775
4.0		-37.781	-37.823	-37.769
5.0	-37.743		-37.803	-37.760
6.0	-37.748	-37.770		
7.0			-37.797	-37.754
10.0		-37.769	-37.797	-37.753

atoms, given by Clementi[24] as -37.792(a.u.). [The experimental value[9] is -37.933(a.u.).] Figure 2 displays the CH^+ curves after these adjustments are made, and after the separated-atom energy has been subtracted.

Using Clementi's[24] radial wave function for $C^+(2p)$ we calculate

$$\langle r_{2p}^2 \rangle = 2.689\, a_o^2 , \tag{3.1}$$

in agreement with Callaway and Dugan.[16] The spherical term of the long-range potential W_o, obtained with (3.1), is also shown in Figure 2 for comparison.

In the numerical computations the CH^+ potentials are matched at $R_m = 6.0$, viz.

$$V_{\Lambda S}(6.0) \equiv W_o(6.0) = -0.00216 \text{ a.u.} , \tag{3.2}$$

for all Λ and S. To do this, a linear fit is provided for each potential between its adjusted value at $R = 5.0$ and the match point. For $R < 5.0$ a numerical interpolation scheme involving Lagrange's interpolating polynomial is used to obtain the values of the potentials at each integration point. The values at a few points are given in TABLE III-2.

The sensitivity of the computed cross sections to the choice of R_m

Figure 2. The CH^+ potential energy curves $^1\Sigma^+$, $^3\Sigma^+$, $^1\Pi$, $^3\Pi$ (from Refs. 21 and 22). The theoretical value of the separated-atom energy, -37.792 a.u., has been subtracted so that all curves asymptotically approach zero at infinite separation. The spherical part of the long-range electrostatic interaction, W_0, is shown for comparison.

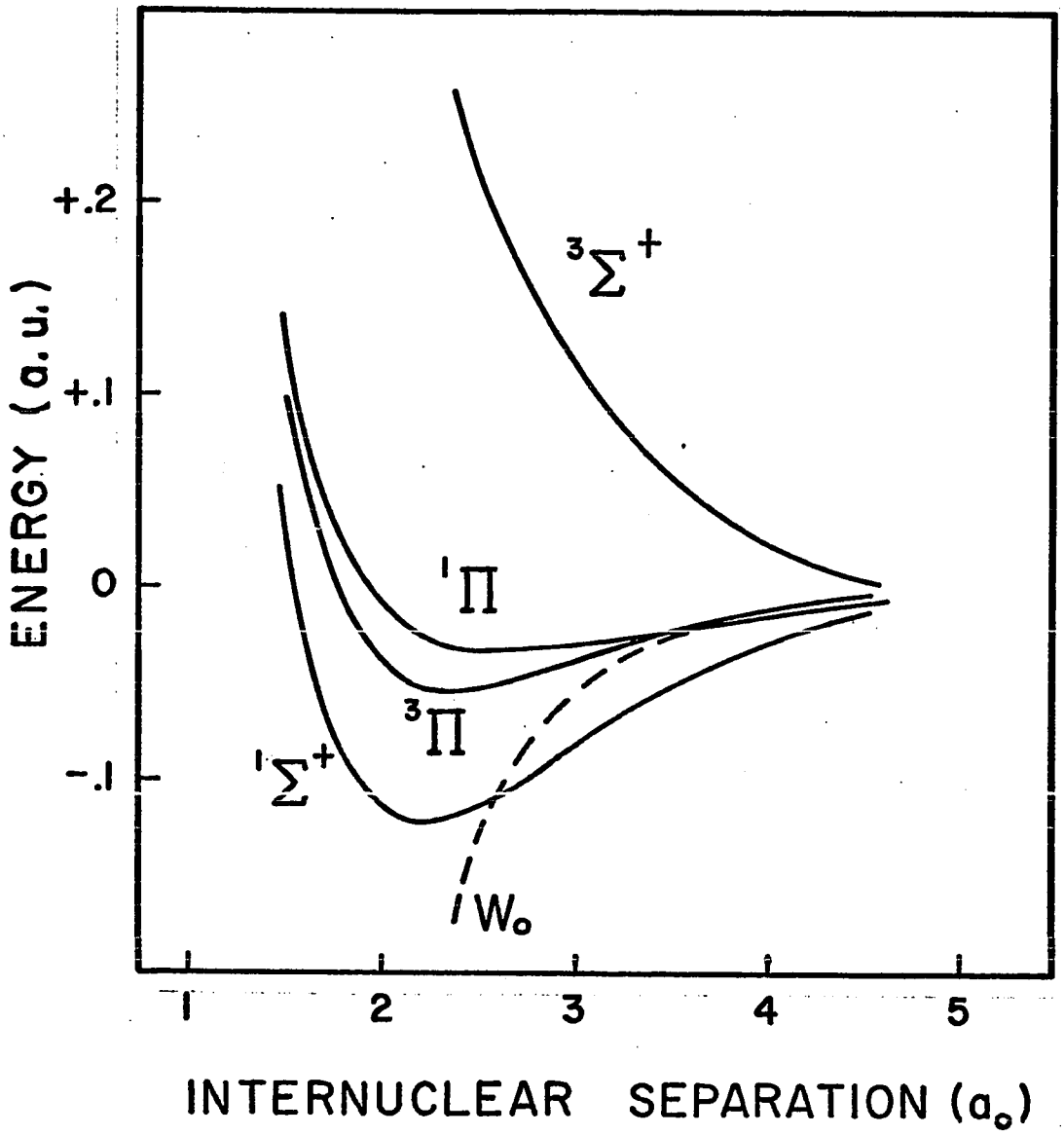
+.2
+.1
0
-.1
ENERGY (a.u.)
$^3\Sigma^+$
$^1\Pi$
$^3\Pi$
$^1\Sigma^+$
W_o
1
2
3
4
5
INTERNUCLEAR SEPARATION (a_o)

TABLE III-2. CH^+ potentials matched at R = 6 to the spherical part of the long-range electrostatic interaction W_0.

R(a_0)	$^1\Sigma^+$ (a.u.)	$^3\Sigma^+$ (a.u.)	$^1\Pi$ (a.u.)	$^3\Pi$ (a.u.)
1.4	0.12300	0.72400	0.20400	0.18300
1.5	0.05372	0.68521	0.13664	0.11240
1.6	-0.00114	0.63324	0.08610	0.05949
1.7	-0.04309	0.57562	0.04886	0.02067
1.8	-0.07386	0.51725	0.02198	-0.00710
1.9	-0.09525	0.46116	0.00302	-0.02632
2.0	-0.10900	0.40900	-0.01000	-0.03900
2.1	-0.11671	0.36152	-0.01865	-0.04679
2.2	-0.11977	0.31887	-0.02416	-0.05099
2.3	-0.11939	0.28083	-0.02746	-0.05261
2.4	-0.11654	0.24703	-0.02924	-0.05241
2.5	-0.11200	0.21700	-0.03000	-0.05100
2.6	-0.10637	0.19030	-0.03007	-0.04879
2.7	-0.10009	0.16655	-0.02969	-0.04611
2.8	-0.09347	0.14541	-0.02900	-0.04315
2.9	-0.08673	0.12663	-0.02809	-0.04008
3.0	-0.08000	0.11000	-0.02700	-0.03700
3.1	-0.07338	0.09536	-0.02578	-0.03397
3.2	-0.06693	0.08258	-0.02444	-0.03102
3.3	-0.06069	0.07152	-0.02301	-0.02820
3.4	-0.05470	0.06204	-0.02152	-0.02552
3.5	-0.04900	0.05400	-0.02000	-0.02300
3.6	-0.04362	0.04722	-0.01848	-0.02064
3.7	-0.03860	0.04153	-0.01699	-0.01846
3.8	-0.03397	0.03672	-0.01557	-0.01646
3.9	-0.02977	0.03261	-0.01423	-0.01464
4.0	-0.02600	0.02900	-0.01300	-0.01300
4.1	-0.02267	0.02573	-0.01187	-0.01153
4.2	-0.01975	0.02266	-0.01083	-0.01021
4.3	-0.01720	0.01971	-0.00985	-0.00904
4.4	-0.01497	0.01682	-0.00892	-0.00797
4.5	-0.01300	0.01400	-0.00800	-0.00700
4.6	-0.01121	0.01128	-0.00705	-0.00610
4.7	-0.00954	0.00873	-0.00607	-0.00525
4.8	-0.00795	0.00645	-0.00504	-0.00444
4.9	-0.00643	0.00452	-0.00400	-0.00369
5.0	-0.00500	0.00300	-0.00300	-0.00300
5.1	-0.00472	0.00248	-0.00292	-0.00292
5.2	-0.00443	0.00197	-0.00283	-0.00283
5.3	-0.00415	0.00145	-0.00275	-0.00275
5.4	-0.00386	0.00094	-0.00266	-0.00266
5.5	-0.00358	0.00042	-0.00258	-0.00258
5.6	-0.00330	-0.00010	-0.00250	-0.00250
5.7	-0.00301	-0.00061	-0.00241	-0.00241
5.8	-0.00273	-0.00113	-0.00233	-0.00233
5.9	-0.00244	-0.00164	-0.00224	-0.00224
6.0	-0.00216	-0.00216	-0.00216	-0.00216

is discussed later. However, we expect it to be small since the $^1\Sigma^+$, $^1\Pi$ and $^3\Pi$ curves are altered very slightly and the repulsive $^3\Sigma^+$ curve is changed only from the adjusted value of 0.00 at $R=6.0$ to the (attractive value -.00216. Because all four potentials must be attractive in the asymptotic region, this modification of the $^3\Sigma^+$ curve is not unreasonable. In Chapter IV the sensitivity of the computed cross sections to a particular choice for R_m is considered.

As discussed earlier, the $W_2(R)$ term in the long range interaction must be modified in such a way that it rapidly approaches zero for $R < R_m$. To accomplish this we multiply W_2 by the expression $\{1-\exp[-(R/\rho_2)^P]\}$; then in the notation of Chapter II,

$$\tilde{W}_2(R) = W_2(R)\left[1 - e^{-(R/\rho_2)^P}\right] . \qquad (3.3)$$

The value $P=16$, chosen arbitrarily, is used throughout. The sensitivity of the cross sections to difference choices of ρ_2 in the range $6 \le \rho_2 \le 10$ is considered later.

B. Numerical Integration of C^+ - H Scattering Equations

The scattering equations (2.55) have the general form

$$\left[\frac{d^2}{dR^2} - \frac{l_i(l_i+1)}{R^2} + k_i^2\right] f_{ij} = \sum_{k=1}^{N} U_{ik} f_{kj} \quad . \tag{3.4}$$

A numerical algorithm particularly suitable for the solution of the equations (3.4) due to Numerov is described in detail by Hartree.[25] It employs the finite difference relation

$$\delta^2 f_{ij}(R_n) = (\delta R)^2 \left[f_{ij}''(R_n) + \frac{1}{12} \delta^2 (f_{ij}''(R_n)) \right] , \tag{3.5}$$

where

$$\delta R = R_{n+1} - R_n \quad , \tag{3.6}$$

$$f_{ij}'' = \frac{d^2}{dR^2} f_{ij} \quad , \tag{3.7}$$

and

$$\delta^2 (f_{ij}(R_n)) = f_{ij}(R_{n+1}) - 2 f_{ij}(R_n) + f_{ij}(R_{n-1}) \quad , \tag{3.8}$$

R_n and R_{n+1} being successive integration points.

Recasting the equations (3.4) in matrix form we put

$$\mathbf{f}'' = \mathbf{G}\mathbf{f} \tag{3.9}$$

with

$$G_{ij} = U_{ij} + \delta(i,j)\left[\frac{l_i(l_i+1)}{R^2} - k_i^2\right] \tag{3.10}$$

Then using (3.5) - (3.8) it follows that

$$\begin{aligned}\mathbf{f}_{n+1} &= \left[\mathbf{1} - \tfrac{1}{12}(\delta R)^2 \mathbf{G}_{n+1}\right] \\ &\times\left\{\left[2\mathbf{1} + \tfrac{5}{6}(\delta R)^2 \mathbf{G}_n\right]\mathbf{f}_n - \left[\mathbf{1} - \tfrac{1}{12}(\delta R)^2 \mathbf{G}_{n-1}\right]\mathbf{f}_{n-1}\right\}\end{aligned} \tag{3.11}$$

where the subscripts on $\mathbf{f}$ and $\mathbf{G}$ denote particular integration points. Our computer program uses this algorithm to integrate the C^+ - H scattering equations. We observe from (3.11) that specifying the solution matrix $\mathbf{f}$ at the first two integration points R_0 and R_1 allows $\mathbf{f}$ to be determined at any subsequent point R_n by iteration.

Because the CH^+ potentials are highly repulsive at small nuclear separations, the solutions $\mathbf{f}$ are unstable near the origin if l_i and k_i^2 are both small. This may be seen from the argument given by Allison and Burke.[10]

Neglecting the energy and centrifugal barrier term $-k_i^2 + \frac{l_i(l_i+1)}{R^2}$,

for small R the equations (3.4) can be written in the approximate form

$$\frac{d^2}{dR^2} f_{ij} = \sum_k U_{ik} f_{kj} . \tag{3.12}$$

Following Allison and Burke, we diagonalize these equations by the orthogonal transformation

$$\mathbf{f}^D = \mathbf{C}\mathbf{f}, \quad \text{and} \quad \mathbf{U}^D = \mathbf{C}\mathbf{U}\mathbf{C}^{-1}, \tag{3.13}$$

which gives

$$\frac{d^2}{dR^2} f_{ij}^D = U_{ii}^D f_{ij}^D . \tag{3.14}$$

An approximate solution to (3.14) is

$$f_{ij}^D = A_{ij} \exp\left[-(U_{ii}^D)^{1/2} R\right] + B_{ij} \exp\left[+(U_{ii}^D)^{1/2} R\right] . \tag{3.15}$$

It is evident from this result that if the U_{ii}^D are large, by starting the numerical integrations at or near $R = 0$, upon integrating outward the positive exponential term may become quite large. Then, at least numerically, the negative term may be so small that the solutions f_{ij}^D become linearly dependent.

To avoid this numerical difficulty, the solutions f_{ij} must be started at some R-value large enough such that, during the integration, the quantity $G_{ii} = \left[U_{ii} + \frac{l_i(l_i+1)}{R^2} - k_i^2 \right]$ becomes negative - causing the solutions to become oscillatory - before linear independence is lost.

Various schemes were devised for starting the solutions as close to the origin as possible. However, another problem was encountered because of large differences in the diagonal terms U_{ii} at small internuclear separations. A typical case, $J = 10$, even parity channels, is illustrated in Figure 3; shown are the six "effective" potentials

$$U_i = U_{ii} + l_i(l_i+1)/R^2 \qquad (3.16)$$

For energies of interest in this paper $k_o^2 \sim 1$, resulting in significantly different classical turning points for the scattering channels. Thus, for example, if all solutions are started at $R_o = 2$, f_{1j} and f_{5j} soon dominate the coupling terms on the R. H. S. of (3.4) and the overall accuracy of the solutions decreases drastically.

Both of the problems discussed above are minimized by starting each solution f_{ij} separately at $R_o(i)$ when the diagonal term becomes less than some prescribed value, coded as USTART. For consistency the solutions f_{kj} generated through the off-diagonal coupling terms are re-set to zero at each integration point as long as

Figure 3. The effective potentials (a.u.) $U_i = U_{ii} + l_i(l_i+1)/R^2$ for the scattering channels $(|i\rangle = |j_i l_i s_i J\rangle)$:

$|1\rangle = |3/2, 12, 21/2, 10\rangle$, $|2\rangle = |3/2, 10, 21/2, 10\rangle$,
$|3\rangle = |1/2, 10, 21/2, 10\rangle$, $|4\rangle = |3/2, 10, 19/2, 10\rangle$,
$|5\rangle = |3/2, 8, 19/2\ 10\rangle$, $|6\rangle = |1/2, 10, 19/2, 10\rangle$.

Note the large differences in the classical turning points for incident energies $k_o^2 \sim 1$.

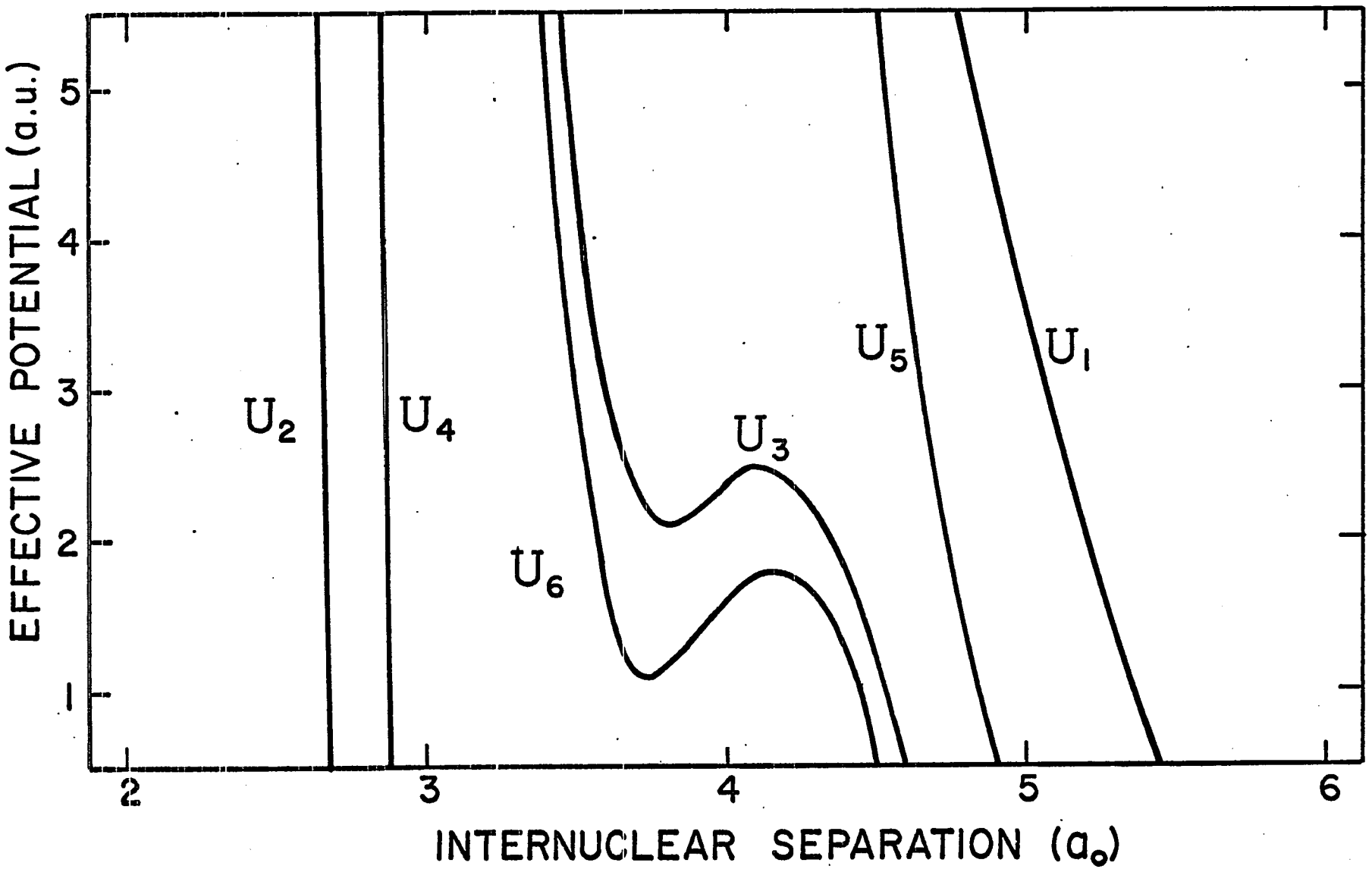
EFFECTIVE POTENTIAL (a.u.)
1
2
3
4
5
2
3
4
5
6
INTERNUCLEAR SEPARATION (a_o)
U_1
U_2
U_3
U_4
U_5
U_6

$U_k >$ USTART.

It is found that for $l_i \lesssim 8$ and $k_i^2 \sim 1$ USTART can be chosen as large as 50. For higher partial waves smaller values of USTART are used. This is because these U_i are dominated by the slowly changing centrifugal terms $l_i(l_i+1)/R^2$, which again allow the solutions to become too large before they begin oscillating. The sensitivity of our results to specific choices for USTART is examined in Chapter IV.

Once the starting point for each channel is determined, the first values assigned each solution are

$$\begin{aligned} x_{ij}(R_0(i)) &= 0 , \\ x_{ij}(R_1(i)) &= c\,\delta(i,j), \end{aligned} \tag{3.17}$$

where c is some constant and the Kronecker delta function is used to insure, ab initio, N linearly independent solutions - one for each possible set of initial quantum numbers.[14,26] We use the notation x_{ij} to indicate that solutions obtained by starting the integration in the manner described do not have the same asymptotic form as the f_{ij} (see Equation (2.17). In the next section we show how the R-matrix may be obtained from the matrix of solutions $\mathbf{X}$.

The numerical integrations were performed with several different choices of step-sizes. It was found that the scheme

$$\delta R = 0.01 \ , \quad \text{for} \quad 1.4 \leq R \leq 6.4 \ ,$$
$$\delta R = 0.02 \ , \quad \text{for} \quad 6.4 < R \leq 26.4 \ ,$$
$$\delta R = 0.16 \ , \quad \text{for} \quad 26.4 < R \leq R_{max} \ ,$$

produced satisfactory results at all energies considered. These step sizes corresponded to approximately 1/20 of the average effective de Broglie wave length in each region,

$$\lambda_{DB}^{eff} = \frac{2\pi}{\left\{ |k_i^2 - U_i| \right\}^{1/2}} \ . \tag{3.18}$$

The use of smaller step sizes did not change the cross sections significantly, and only increased both computation time and numerical error. The integrations were carried out to $R_{max} = 155$. For the lowest energies considered, $R_{max} = 125$ was sufficient to provide convergence of the results.

C. Evaluation of the $\mathbb{R}$-Matrix

The asymptotic form of the solutions f_{ij} is given in terms of the scattering $\mathbb{S}$-matrix elements by Equation (2.17). In practice it is more convenient to deal with real solutions,[26] in which case we put

$$f_{ij}(R) \underset{R\to\infty}{\sim} \delta(i,j)\sin(k_i R - \ell_i\pi/2) + (k_j/k_i)^{1/2}(\mathbb{R})_{ij}\cos(k_i R - \ell_i\pi/2) . \tag{3.19}$$

The $\mathbb{R}$-matrix elements defined by (3.19) are related to the $\mathbb{S}$-matrix elements by

$$\mathbb{S} = (\mathbb{1} + i\mathbb{R})(\mathbb{1} - i\mathbb{R})^{-1} . \tag{3.20}$$

Further, the $\mathbb{R}$-matrix may be shown to be real and symmetric.[13]

The asymptotic form of the solutions $\mathbb{X}$ may be used to calculate the $\mathbb{R}$-matrix. The procedure given here is due to Lane and Geltman.[14]

For large internuclear separations we may write

$$\underset{(\text{large } R)}{\mathbb{X}(R)} = \mathbb{A}_1\,\mathbb{J}(R) + \mathbb{A}_2\,\mathbb{N}(R) , \tag{3.21}$$

where

$$\left(\mathbb{J}(R)\right)_{\alpha\beta} = \delta(\alpha,\beta)\left[k_\alpha R\right] j_{l_\alpha}(k_\alpha R), \tag{3.22}$$

and

$$\left(\mathbb{N}(R)\right)_{\alpha\beta} = -\delta(\alpha,\beta)\left[k_\alpha R\right] n_{l_\alpha}(k_\alpha R). \tag{3.23}$$

The functions j_{l_α} and n_{l_α} are spherical Bessel functions of the first and second kind,[27] respectively, and $\mathbb{A}_1$ and $\mathbb{A}_2$ are constant matrices. By matching the solution matrix $\mathbb{X}$ to the asymptotic form (3.21) at two large R -values, say R_a and R_b, we find

$$\mathbb{A}_1 = \mathbb{B}^{-1}\left[\mathbb{N}(R_b)\mathbb{X}(R_a) - \mathbb{N}(R_a)\mathbb{X}(R_b)\right], \tag{3.24}$$

and

$$\mathbb{A}_2 = \mathbb{B}^{-1}\left[\mathbb{J}(R_b)\mathbb{X}(R_a) - \mathbb{J}(R_a)\mathbb{X}(R_b)\right], \tag{3.25}$$

where

$$\mathbb{B} = \left[\mathbb{N}(R_b)\mathbb{J}(R_a) - \mathbb{N}(R_a)\mathbb{J}(R_b)\right]. \tag{3.26}$$

Then, defining the momentum matrix $\mathbb{K}$ with elements

$$(\mathbb{K})_{\alpha\beta} = \delta(\alpha,\beta)\, k_\alpha \ , \tag{3.27}$$

it follows that the $\mathbb{R}$-matrix is given by

$$\mathbb{R} = \mathbb{K}^{1/2}\left(\mathbb{A}_2\mathbb{A}_1^{-1}\right)\mathbb{K}^{-1/2}. \tag{3.28}$$

Once the $\mathbb{R}$-matrix has been obtained for a particular set of coupled equations, i.e. specific J, k_o^2 and parity, the $\mathbf{S}$- and $\mathbf{T}$-matrices may be computed and the partial cross sections then calculated in a straight foreward manner from the relations given in Chapter II, Section B.

D. General Description of the Computer Code

The main program utilizes several subroutines which:

1. read in the initial data containing the energies, parities and angular momenta J to be considered, the values assigned to USTART and ρ_2, the parameters specifying the long range potentials W_λ, and the coupling terms to be considered (i.e. spin-change only, rotational only, or both);
2. read in the integration step sizes and number of steps and then determine all integration points R_n;
3. determine sets of boundary matching points (R_a, R_b);
4. calculate the molecular curves $U_{\Lambda S}$ for all $R_n \leq R_m$;
5. assign values of j, l, and η to each channel; and
6. calculate the coupling matrices $q_{\lambda\lambda}$ and $P^J_{\Lambda S}$ if required.

Next the main program begins the integration algorithm, which is then iterated in another subroutine. As solutions are obtained at sets of boundary matching points, an additional subroutine is called to calculate the R- , S- , and T- matrices, compute partial cross sections for each channel and then sum these to obtain the partial cross sections $Q(1/2, 1/2)$, $Q(1/2, 3/2)$, $Q(3/2, 1/2)$, $Q(3/2, 3/2)$ for a given J , k_0^2 and parity.

The 3-j and 6-j symbols necessary for the evaluation of the

coupling coefficients, and the spherical Bessel functions used in the calculation of the $\mathbb{R}$ -matrix are generated by the program. These subroutines were checked extensively against existing tables.[17,27]

All computations were performed on the University of Texas (Austin) Control Data Corporation 6600 computer. Typically, the time required to obtain the C^+ - H partial cross sections for a given J, k_o^2 and parity was 40 seconds; after the potentials had been calculated, subsequent integrations of the coupled equations required approximately 35 seconds.

IV. RESULTS AND CONCLUSIONS

A. C^+ - H Elastic and Fine-Structure Excitation Cross Sections

The C^+ - H scattering equations were solved for seven center-of-mass energies E_o ranging from .0100 ev to .0850 ev. These values and the corresponding values of k_o^2 (a.u.) and the effective temperature $T(°K) = E_o/k_B$, are listed in TABLE IV. 1. The $C^+(^2P_{1/2}) \rightarrow C^+(^2P_{3/2})$ excitation threshold is also given for reference.

Because the numerical integrations require considerable computation time, at each energy considered the scattering equations are solved for channels of both parities but only even $J \leq 30$(denoted $J = 0(2)30$), and $J = 35, 40, 45, 50$ (denoted $J = 35(5)50$). Now for $J=0$, there are just two channels for a given parity, for $J=1$, five channels, and for $J \geq 2$, six channels. Consequently, the prescription we use to estimate the total cross sections for the $j \Rightarrow i$ transition is

$$Q_{ij} = Q_{ij}(0^+) + Q_{ij}(0^-) + 2 \sum_{J=2(2)30} \left[Q_{ij}(J^+) + Q_{ij}(J^-) \right] + 5 \sum_{J=35(5)50} \left[Q_{ij}(J^+) + Q_{ij}(J^-) \right] , \quad (4.1)$$

where $Q(J^+)$ and $Q(J^-)$ correspond to the sum of the partial cross sections of, respectively, even and odd parity channels having the

TABLE IV-1. Center-of-mass energies for C^+ - H Collisions

E_o (ev)	k_o^2 (a.u.)	T (°K)
($\Delta E_o = .0079$)	($\Delta k_o^2 = .9961$)	($\Delta T = 92.1$)
.0100	1.255	116.0
.0125	1.569	145.0
.0150	1.882	174.1
.0175	2.196	203.1
.0275	3.451	319.1
.0500	6.275	580.0
.0850	10.67	986.4

total angular momentum J .

To determine the accuracy of this procedure for $k_o^2 = 1.255$ we also solve the scattering equations for $J^{\pm} = 1(2)19$, and appropriately modify Equation (4. 1) to obtain the total cross sections.

The total cross sections at each energy, as calculated by the (correct) Equation (4. 1), are given in TABLE IV-2. The notation (j', j) represents the $C^+(^2P_j) \Rightarrow C^+(^2P_{j'})$ cross section. We find that for $k_o^2 = 1.255$, the excitation cross sections

$$Q_{3/2,1/2}^{(\text{even } J)} = \sum_{J=2(2)20} \left[Q_{3/2,1/2}(J^+) + Q_{3/2,1/2}(J^-) \right] = 88.4\ a_o^2 ,$$

and

$$Q_{3/2,1/2}^{(\text{odd } J)} = \sum_{J=1(2)19} \left[Q_{3/2,1/2}(J^+) + Q_{3/2,1/2}(J^-) \right] = 84.9\ a_o^2 .$$

The difference between these two values is a measure of the error introduced by estimating the total cross sections using the prescription described above.

All of the partial cross section computed to be greater than .01 a_o^2 are listed in TABLES IV-3 to IV-9. We have also plotted in Figures 4-10 both even (+) and odd (-) parity partial cross sections for the excitation process $(3/2, 1/2)$ at each energy considered. As k_o^2 increases we see that more partial waves contribute to the total cross

TABLE IV-2. C^+ - H total cross sections (a_o^2)

k_o^2	(½,½)	(½,3/2)	(3/2,½)	(3/2,3/2)
1.255	2478.	417.2	174.0	3989.
1.569	2271.	268.4	196.0	3174.
1.882	2138.	210.2	198.4	2571.
2.196	2055.	165.8	181.1	2462.
3.451	1623.	110.5	157.0	1986.
6.275	1305.	68.7	115.6	1442.
10.67	1177.	56.5	102.4	1392.

TABLE IV-3. C^+ - H partial cross sections (a_0^2) at $k_0^2 = 1.255$.

J		(1/2, 1/2)	(1/2, 3/2)	(3/2, 1/2)	(3/2, 3/2)
0	+	.5943	.8227	.3395	2.110
	-	1.807	.7553	.3116	3.968
1	+	4.003	7.794	3.217	23.56
	-	4.573	6.368	2.628	17.58
2	+	5.926	9.401	3.880	57.52
	-	10.09	8.186	3.383	23.88
3	+	19.24	8.602	3.572	89.76
	-	5.799	13.19	5.444	67.52
4	+	21.15	19.68	8.120	92.95
	-	11.72	11.78	4.870	94.07
5	+	23.36	16.63	6.868	81.48
	-	19.20	25.67	10.59	117.1
6	+	21.79	30.00	12.38	110.4
	-	33.06	22.45	9.378	113.2
7	+	37.31	27.16	11.84	136.9
	-	30.28	31.68	13.08	222.4
8	+	36.57	27.74	12.44	174.9
	-	38.72	23.10	9.547	272.2
9	+	44.16	27.74	15.17	211.5
	-	25.28	24.15	9.971	283.6
10	+	29.90	30.30	12.50	193.2
	-	38.84	28.10	12.64	268.1
11	+	91.14	1.964	.8183	210.8
	-	77.76	4.169	1.720	235.0
12	+	63.94	.7114	.2948	151.7
	-	76.63	$< 10^{-2}$	$< 10^{-2}$	129.4

TABLE IV-3 (continued)

J		(½,½)	(½, 3/2)	(3/2, ½)	(3/2, 3/2)
13	+	100.8			82.28
	-	23.64			95.20
14	+	121.5			61.75
	-	80.66			54.62
15	+	125.6			38.59
	-	158.2			41.75
16	+	121.4			29.24
	-	126.4			26.98
17	+	92.96			19.89
	-	94.08			21.08
18	+	72.04			15.53
	-	78.28			14.55
19	+	57.51			10.99
	-	55.35			11.68
20	+	42.92			8.904
	-	40.42			8.452
22	+	26.46			5.408
	-	27.93			5.172
24	+	17.13			3.512
	-	17.75			3.387
26	+	11.39			2.326
	-	11.75			2.254
28	+	7.754			1.588
	-	7.980			1.544
30	+	5.451			1.111
	-	5.586			1.085

TABLE IV-3 (continued)

J		(½,½)	(½,3/2)	(3/2,½)	(3/2,3/2)
35	+	2.568			.4889
	-	2.525			.4969
40	+	1.301			.2440
	-	1.316			.2406
45	+	.6968			.1267
	-	.6961			.0862

TABLE IV-4. C^+ - H partial cross sections (a_0^J) at $k_0^2 = 1.569$.

J		(½, ½)	(½, 3/2)	(3/2, ½)	(3/2, 3/2)
0	+	1.423	.3604	.2632	.067
	-	.4089	.3070	.2261	1.850
2	+	11.56	4.033	2.946	17.80
	-	1.744	3.662	2.670	27.89
4	+	7.540	8.496	6.206	40.52
	-	17.86	5.059	3.678	34.94
6	+	16.55	13.84	10.10	39.83
	-	21.71	9.836	7.168	76.64
8	+	28.82	15.04	10.98	90.71
	-	33.28	13.68	9.977	93.38
10	+	30.98	14.04	10.25	94.88
	-	23.55	23.48	17.15	124.2
12	+	75.08	6.559	4.790	171.2
	-	31.82	16.12	11.78	163.8
14	+	9.014	.0510	.0478	140.2
	-	99.16	$<10^{-2}$	$<10^{-2}$	128.5
16	+	128.2			69.52
	-	93.36			87.55
18	+	87.10			36.57
	-	89.04			32.15
20	+	53.54			20.64
	-	55.94			19.50
22	+	33.45			12.45
	-	34.88			12.90
24	+	21.61			7.971
	-	22.44			7.684

TABLE IV-4 (continued)

J		(½, ½)	(½, 3/2)	(3/2, ½)	(3/2, 3/2)
26	+	14.44			5.289
	-	14.90			5.128
28	+	9.941			3.625
	-	10.20			3.529
30	+	6.975			2.552
	-	7.144			2.493
35	+	3.232			1.146
	-	3.176			1.166
40	+	1.635			.5912
	-	1.657			.5831
45	+	.9210			.3197
	-	.9115			.3234
50	+	.5400			.1874
	-	.5444			.1806

TABLE IV-5. C^+ - H partial cross sections (a_o^2) at $k_o^2 = 1.882$.

J		(½, ½)	(½, 3/2)	(3/2, ½)	(3/2, 3/2)
0	+	.6752	.2262	.2130	1.280
	-	.1188	.1806	.1701	.1560
2	+	7.114	2.577	2.332	20.56
	-	6.810	2.349	2.215	11.59
4	+	4.053	5.211	4.906	23.39
	-	17.11	3.099	2.918	37.30
6	+	14.63	9.047	8.518	32.25
	-	21.04	6.093	5.762	24.37
8	+	23.65	9.922	9.341	52.27
	-	21.41	8.610	8.109	43.18
10	+	32.37	11.47	10.79	22.12
	-	24.39	14.35	13.08	49.31
12	+	49.52	13.08	12.32	74.56
	-	44.02	11.24	11.05	128.2
14	+	14.12	7.171	6.751	109.7
	-	87.70	6.051	7.341	159.4
16	+	48.72	.1282	.1791	104.4
	-	86.35	$< 10^{-2}$	$< 10^{-2}$	98.63
18	+	97.28			57.89
	-	97.02			54.36
20	+	63.15			33.18
	-	65.59			31.46
22	+	40.15			20.00
	-	41.74			19.12
24	+	26.14			12.63
	-	27.08			12.15

TABLE IV-5 (continued)

J		(½,½)	(½,3/2)	(3/2,½)	(3/2,3/2)
26	+	17.51			8.295
	-	18.04			8.031
28	+	12.04			5.665
	-	12.37			5.515
30	+	8.502			3.988
	-	8.701			3.896
35	+	3.931			1.798
	-	3.858			1.828
40	+	1.974			.9312
	-	2.000			.9195
45	+	1.113			.5082
	-	1.102			.5133
50	+	.6542			.3006
	-	.6509			.2983

TABLE IV-6. C^+ - H partial cross sections (a_o^2) at $k_o^2 = 2.196$.

J		(1/2, 1/2)	(1/2, 3/2)	(3/2, 1/2)	(3/2, 3/2)
0	+	.0466	.1625	.1776	.1372
	-	.8122	.1192	.1302	.6613
2	+	1.752	1.739	1.902	5.470
	-	9.496	1.724	1.886	18.64
4	+	10.40	3.634	3.972	23.68
	-	8.331	2.189	2.393	14.19
6	+	10.76	6.672	7.291	30.02
	-	11.91	4.354	4.742	33.00
8	+	17.22	7.398	8.085	32.20
	-	10.09	6.314	6.895	39.24
10	+	29.73	8.956	9.788	38.92
	-	20.18	10.06	11.00	35.28
12	+	40.35	8.975	9.808	84.24
	-	35.52	10.54	11.51	29.46
14	+	35.54	3.485	3.809	126.3
	-	33.12	6.380	6.983	86.95
16	+	74.65	.2567	.2804	116.2
	-	48.12	.0409	.0447	121.5
18	+	100.1	$< 10^{-2}$	$< 10^{-2}$	76.84
	-	92.35			73.04
20	+	71.27			45.36
	-	73.03			43.12
22	+	46.51			27.62
	-	48.16			26.44
24	+	30.57			17.56
	-	31.62			16.93

TABLE IV-6 (continued)

J	$(1/2, 1/2)$	$(1/2, 3/2)$	$(3/2, 1/2)$	$(3/2, 3/2)$
26^+	20.56			11.55
26^-	21.18			11.18
28^+	14.18			7.815
28^-	14.56			7.509
30^+	10.02			5.457
30^-	10.25			5.325
35^+	4.678			2.452
35^-	4.600			2.494
40^+	2.322			1.274
40^-	2.354			1.257
45^+	1.309			.6970
45^-	1.296			.7042
50^+	.7706			.4143
50^-	.7769			.4108

TABLE IV-7. C^+ - H partial cross sections (a_o^2) at $k_o^2 = 3.451$.

J		(1/2, 1/2)	(1/2, 3/2)	(3/2, 1/2)	(3/2, 3/2)
0	+	.5109	.07351	.1046	.3332
	-	.0093	.0313	.0446	.4415
2	+	5.439	.7072	1.006	2.109
	-	2.436	.8329	1.186	9.278
4	+	1.194	1.428	2.032	11.91
	-	11.26	1.024	1.457	6.221
6	+	10.84	2.974	4.232	11.82
	-	6.690	1.894	2.694	15.59
8	+	7.544	3.722	5.295	17.55
	-	13.68	3.102	4.412	14.01
10	+	8.537	4.306	6.126	27.32
	-	13.88	4.343	6.180	20.18
12	+	10.42	4.930	7.014	30.63
	-	16.92	5.027	7.150	22.38
14	+	17.39	4.718	6.712	47.80
	-	23.62	6.024	8.568	37.40
16	+	2.226	3.882	5.522	41.34
	-	20.60	3.229	4.595	31.78
18	+	32.76	.9209	1.310	79.47
	-	26.74	2.263	3.375	67.23
20	+	74.53	.0294	.0418	76.22
	-	64.00	.0104	.0472	77.00
22	+	64.45	$<10^{-2}$	$<10^{-2}$	54.42
	-	64.37			52.96
24	+	46.26			36.37
	-	47.26			35.25

TABLE IV-7 (continued)

J		(1/2, 1/2)	(1/2, 3/2)	(3/2, 1/2)	(3/2, 3/2)
26	+	32.24			24.44
	-	33.06			23.74
28	+	27.62			16.79
	-	23.17			16.36
30	+	16.14			11.81
	-	16.50			11.54
35	+	7.514			5.282
	-	7.507			5.374
40	+	3.860			2.701
	-	3.912			2.663
45	+	2.170			1.473
	-	2.148			1.488
50	+	1.265			.8827
	-	1.276			.8756

TABLE IV-8. C^+ - H partial cross sections (a_0^2) at $k_0^2 = 6.275$.

J		(½, ½)	(½, 3/2)	(3/2, ½)	(3/2, 3/2)
0	+	.2297	.0252	.0423	.1442
	-	.0331	$< 10^{-2}$	$< 10^{-2}$	.2086
2	+	.2867	.1938	.3308	3.503
	-	1.535	.3538	.5955	1.851
4	+	.4562	.4364	.7342	7.241
	-	5.868	.6296	1.057	2.569
6	+	6.623	.9991	1.681	4.902
	-	2.648	1.029	1.734	9.100
8	+	9.102	1.552	2.610	8.896
	-	3.159	1.616	2.717	8.957
10	+	5.054	1.699	2.858	12.15
	-	7.434	1.692	2.846	16.70
12	+	6.311	2.016	3.392	11.64
	-	6.996	2.845	4.787	15.48
14	+	11.66	2.874	4.835	5.722
	-	5.273	2.988	5.027	7.545
16	+	9.612	2.861	4.814	10.76
	-	4.372	4.005	6.739	9.715
18	+	10.13	1.422	2.392	6.850
	-	15.67	.7362	1.236	21.33
20	+	30.34	2.208	3.715	24.48
	-	12.36	1.624	2.729	24.39
22	+	12.74	.3133	.5271	37.47
	-	25.45	.1576	.2662	36.59
24	+	48.30	.0489	.0824	50.94
	-	43.64	.0270	.0454	53.35

TABLE IV-8 (continued)

J		(½, ½)	(½, 3/2)	(3/2, ½)	(3/2, 3/2)
26	+	47.21	.0130	.0219	45.04
	-	46.56	$< 10^{-2}$	.0138	44.94
28	+	37.74		$< 10^{-2}$	34.42
	-	38.05			33.92
30	+	28.64			25.45
	-	29.06			25.00
35	+	14.37			11.96
	-	14.15			12.15
40	+	7.458			6.283
	-	7.548			6.204
45	+	4.272			3.480
	-	4.232			3.514
50	+	2.558			2.096
	-	2.579			2.080

TABLE IV-9. C^+ - H partial cross sections (a_0^2) at $k_0^2 = 10.67$.

J		(½, ½)	(½, 3/2)	(3/2, ½)	(3/2, 3/2)
0	+	.7265	$< 10^{-2}$	$< 10^{-2}$	.1495
	-	.0440	.0158	.0287	$< 10^{-2}$
2	+	1.024	.0745	.1404	2.704
	-	1.006	.1802	.3268	.7292
4	+	.3267	.1500	.2720	2.717
	-	2.496	.4843	.8784	2.447
6	+	4.545	.2802	.5080	2.586
	-	1.762	.7496	1.358	4.082
8	+	3.813	.6827	1.238	5.766
	-	3.528	1.108	2.050	4.797
10	+	5.089	1.312	2.378	5.302
	-	4.215	1.446	2.623	4.064
12	+	5.223	1.569	2.845	3.138
	-	2.432	1.360	2.467	3.711
14	+	3.842	1.200	2.175	5.178
	-	3.274	1.640	2.975	4.186
16	+	5.824	1.938	3.515	8.433
	-	8.553	2.024	3.674	8.953
18	+	15.04	1.589	2.881	16.57
	-	13.01	1.760	3.189	16.05
20	+	14.18	1.994	3.615	18.38
	-	13.88	1.844	3.338	15.40
22	+	23.14	.5618	1.019	19.50
	-	11.14	3.233	5.860	15.98
24	+	13.12	.2408	.4366	14.49
	-	13.10	.4617	.8364	14.84

TABLE IV-9 (continued)

J^{π}	$(1/2, 1/2)$	$(1/2, 3/2)$	$(3/2, 1/2)$	$(3/2, 3/2)$
26^{+}	8.028	.1164	.2111	19.03
26^{-}	10.43	.0917	.1638	18.36
28^{+}	30.38	.0539	.0977	32.73
28^{-}	27.72	.0384	.0697	64.71
30^{+}	35.28	.0207	.0375	35.24
30^{-}	34.40	$<10^{-2}$	$<10^{-2}$	35.75
35^{+}	24.50			22.57
35^{-}	24.33			35.76
40^{+}	14.43			13.09
40^{-}	14.56			22.78
45^{+}	8.943			7.807
45^{-}	8.875			7.874
50^{+}	5.785			5.037
50^{-}	5.826			5.003

Figure 4. The partial excitation cross sections (a_0^2) for even (+) and odd (-) parity scattering channels, $Q_{3/2,1/2}$ (J^+) and $Q_{3/2,1/2}$ (J^-), are plotted vs. J for the incident energy k_0^2 = 1.255 (.01 ev).

Figure 5. As for Figure 4 for k_0^2 = 1.569 (.0125 ev), but with only even J-values being plotted.

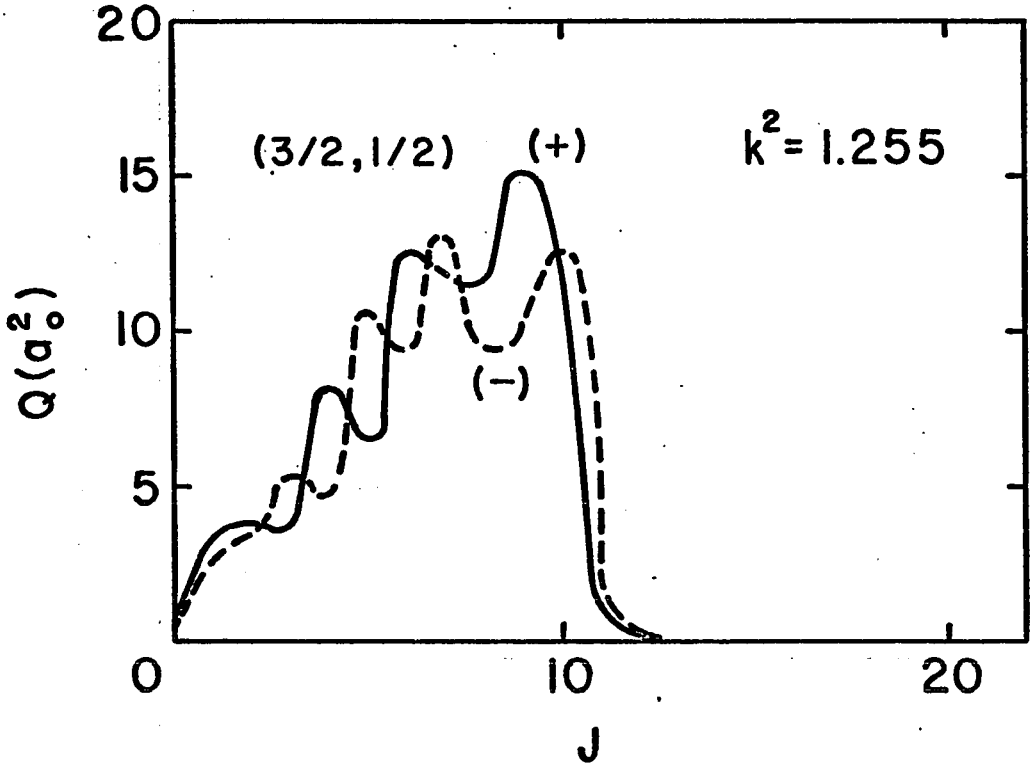
20
15
10
5
0
10
20
J
Q(a₀²)
(3/2,1/2)
(+)
(−)
k² = 1.255

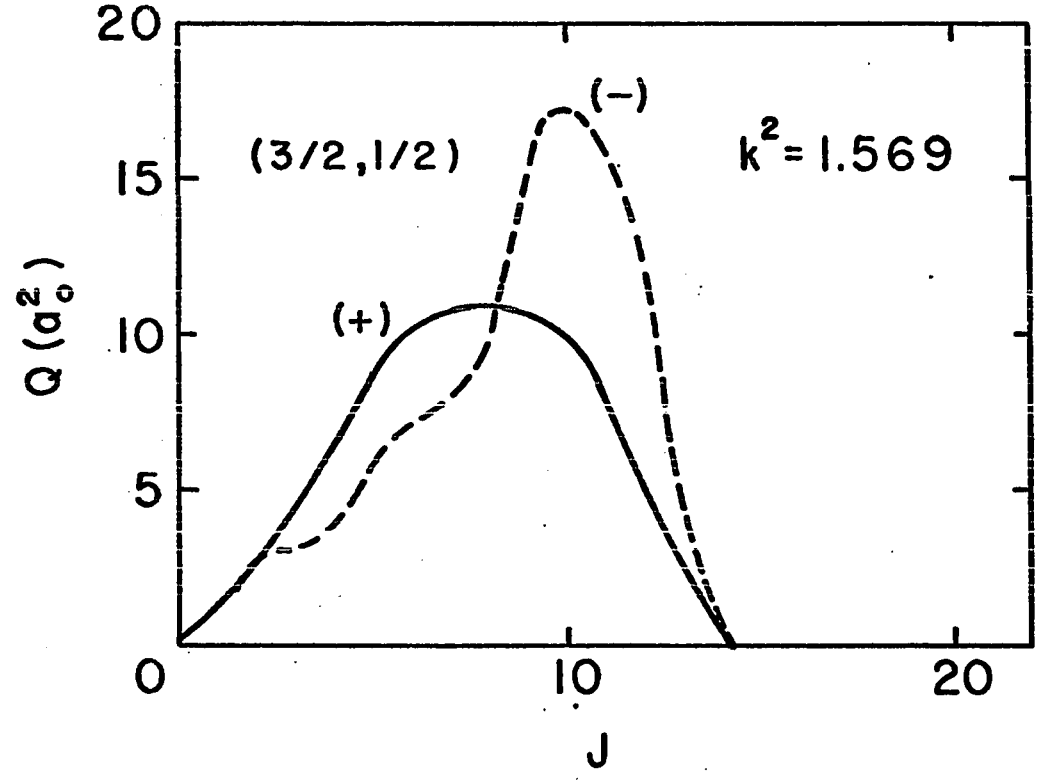
20
15
10
5
0
10
20
J
Q(a₀²)
(3/2,1/2)
(−)
(+)
k² = 1.569

Figures 6 and 7. As for Figure 5 for $k_o^2 = 1.882$ (.015 ev) and $k_o^2 = 2.196$ (.0175 ev).

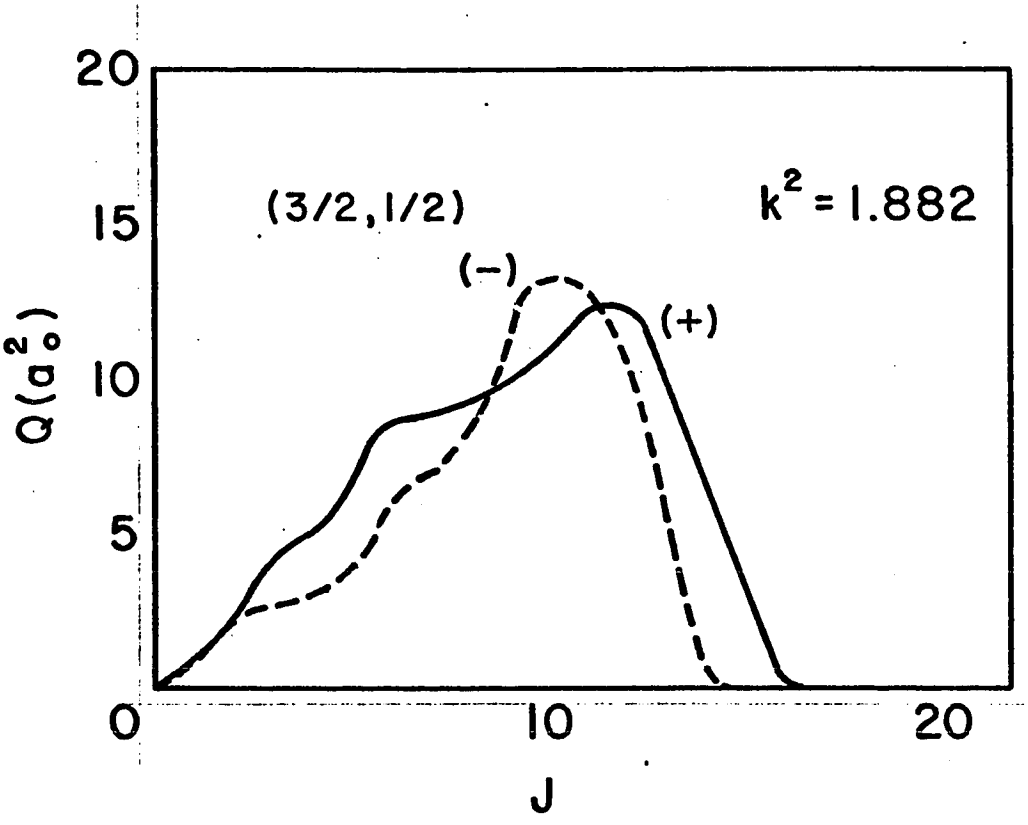
20
15
10
5
0
10
20
J
Q(a₀²)
(3/2,1/2)
k² = 1.882
(−)
(+)

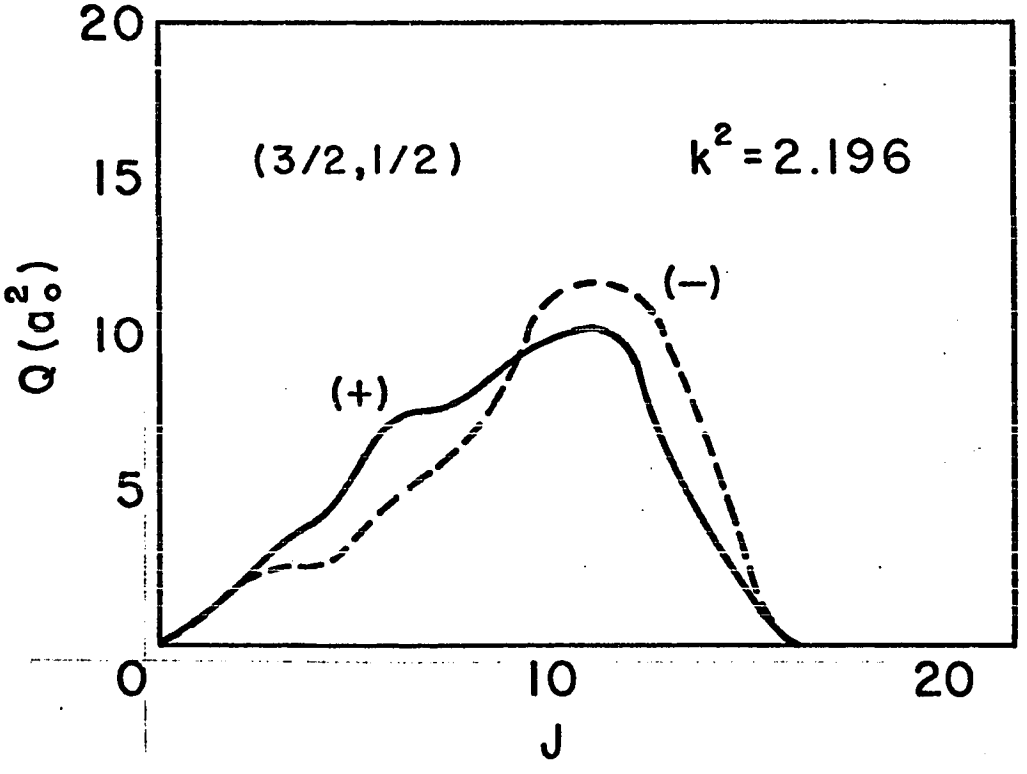
20
15
10
5
0
10
20
J
Q(a₀²)
(3/2,1/2)
k² = 2.196
(−)
(+)

Figures 8 and 9. As for Figure 5 for $k_o^2 = 3.451$ (.0275 ev) and $k_o^2 = 6.275$ (.05 ev).

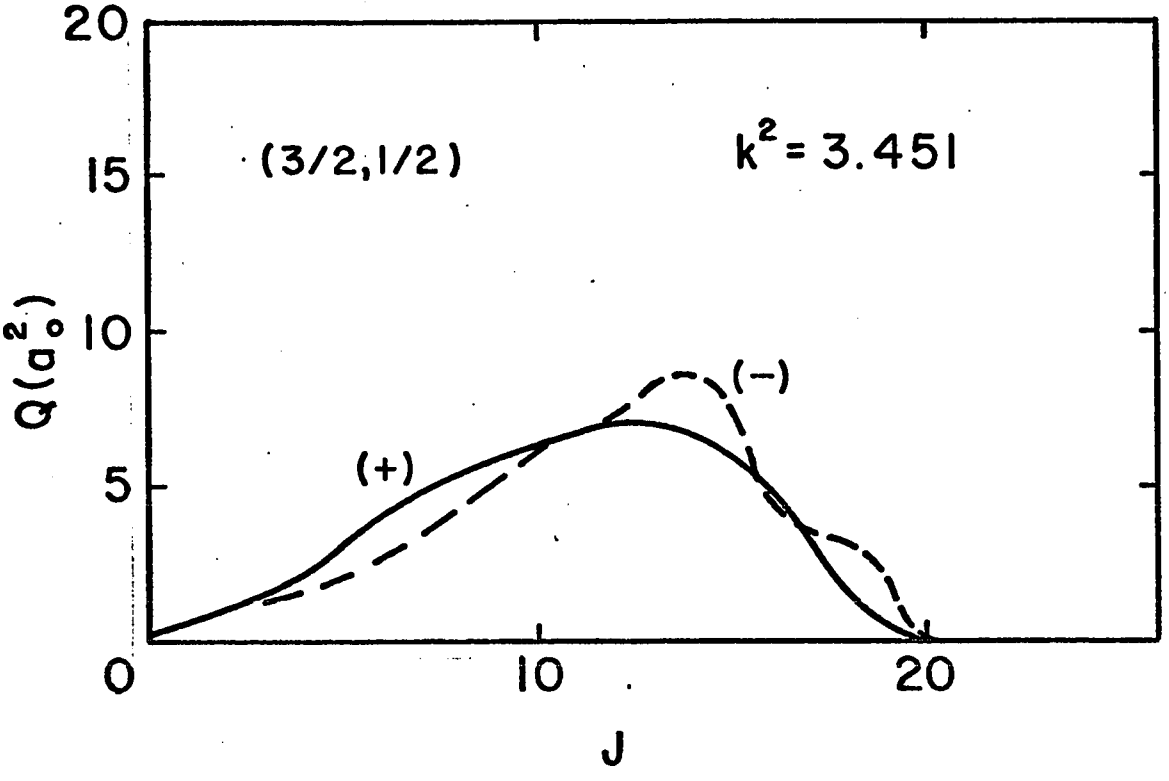
20
15
10
5
0
10
20
J
Q(a₀²)
(3/2,1/2)
k² = 3.451
(+)
(−)

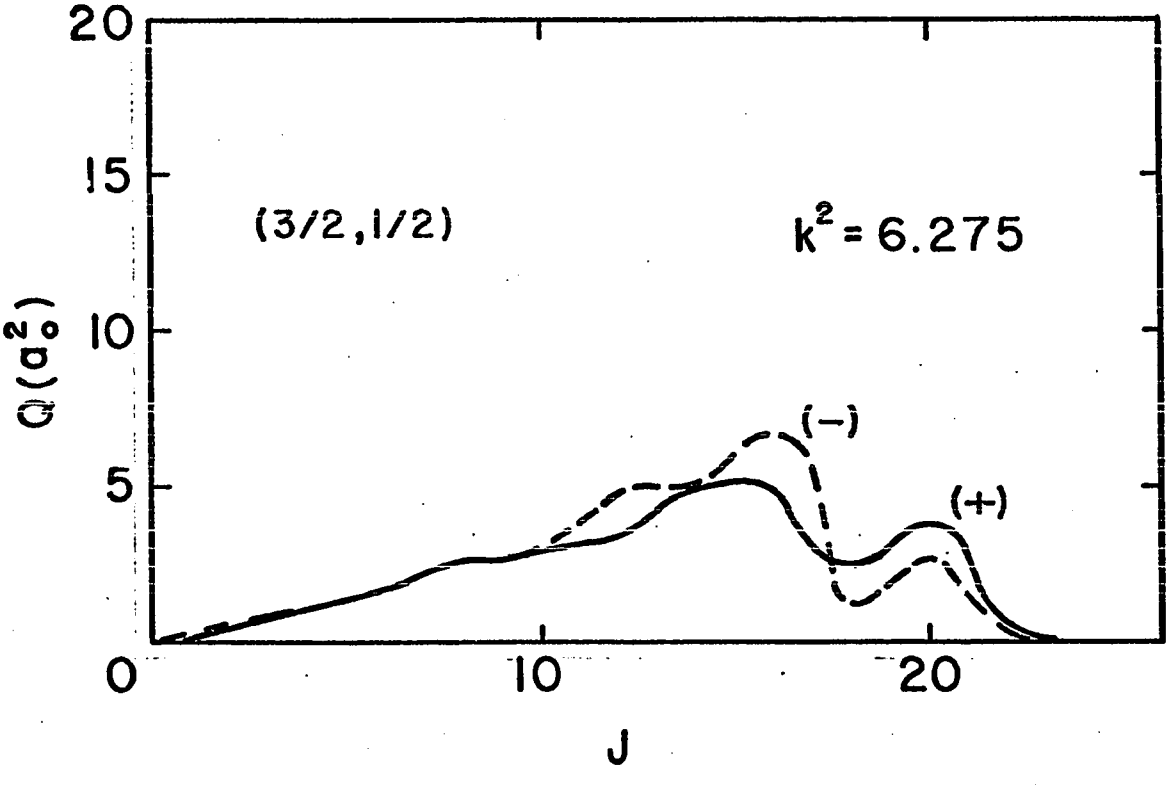
20
15
10
5
0
10
20
J
Q(a₀²)
(3/2,1/2)
k² = 6.275
(−)
(+)

Figure 10. As for Figure 5 for $k_o^2 = 10.67$ (.085 ev).

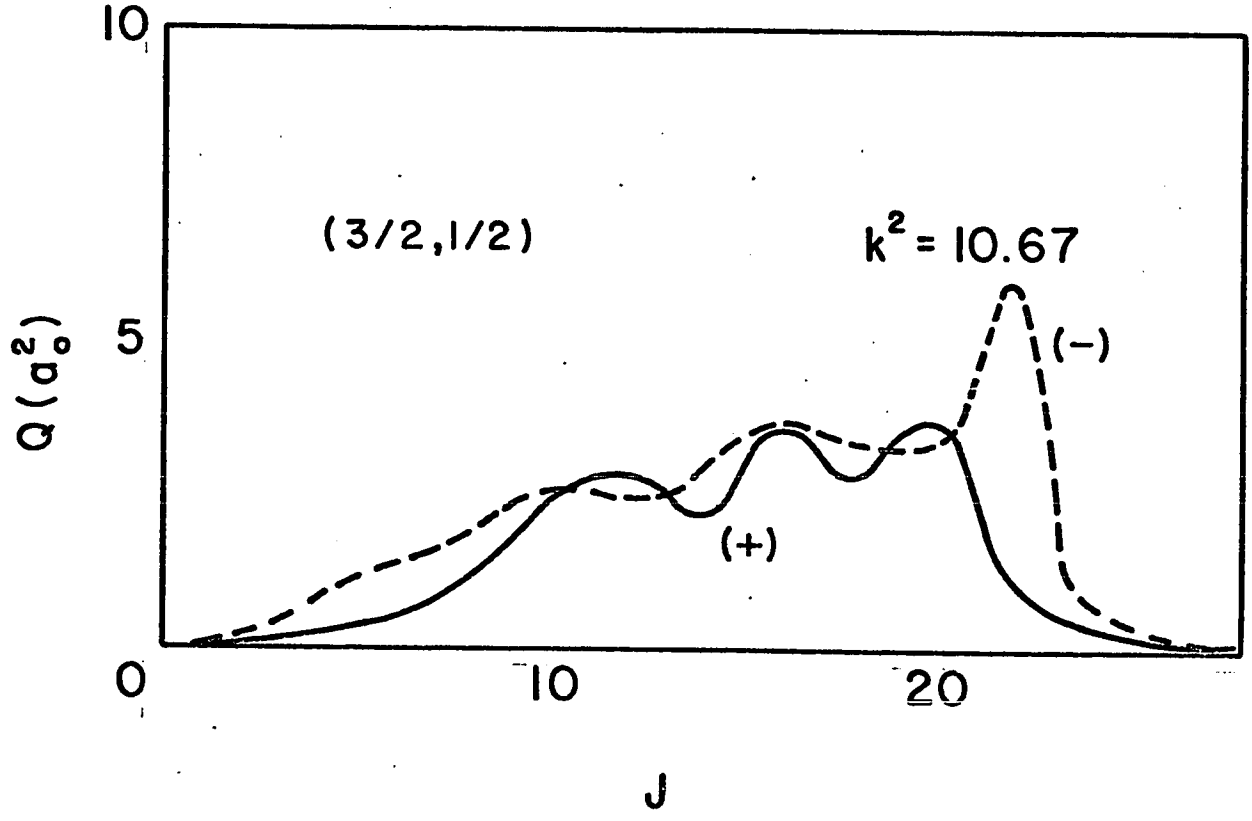
10
5
0
10
20
(3/2,1/2)
$k^2 = 10.67$
(+)
(-)
$Q(a_0^2)$
J

section, and further that the relative contribution from any given $Q(J)$ decreases.

The first observation may be understood by realizing that the classical turning points $R_t(i)$ for the scattering channels (i), defined by

$$k_i^2 = U_{ii}(R_t(i)) + \frac{l_i(l_i+1)}{R_t^2(i)} , \qquad (4.2)$$

decrease as k_i^2 increases. This fact is accounted for in the numerical procedure by using larger values of USTART for higher energies. Now as we show below, the spin-change process provides most of the coupling between the C^+ fine-structure levels, and in the formalism we have used this coupling occurs only for $R < R_m$, the match point. Hence, at higher energies scattering channels with larger l's (and larger J's) can have classical turning points measurably less than R_m, enabling these channels to contribute significantly to the inelastic cross sections.

The second observation reflects the fact that at higher energies the terms

$$G_{ij}(R) = U_{ij}(R) + \delta(i,j)\left[\frac{l_i(l_i+1)}{R^2} - k_i^2\right] , \qquad (3.10)$$

appearing in Equation (3.9), are relatively less sensitive to the

detailed shapes of the coupling quantities U_{ij} in the region beyond the classical turning points $R_t(i)$. The ℓ's for scattering channels of a given parity and J are $\ell = J-2, J, J+2$. Consequently, for larger k^2 the functions f^J and f^{J+1}, say, are solutions of approximately the same scattering equations, and so the partial cross sections $Q(J)$ and $Q(J+1)$ are approximately equal.

As a typical example of a C^+ - H elastic cross section we show in Figure 11 the even and odd parity partial cross sections for the elastic scattering process (½ , ½) at $k_o^2 = 1.255$. The oscillations in $Q(J)$ are similar to those described by Allison and Burke[8] for elastic scattering of $O(^3P)$ by $O(^3P)$.

In Figure 12 we compare our results (w) for the C^+ - H excitation cross section (3/2 , ½) to those reported by Smith,[7] and Callaway and Dugan.[6] We recall that Smith's results (S) are obtained from an orbiting approximation of the elastic spin-change formalism,[10] and do not include the specific forms of the CH^+ potential energy curves. The results of Callaway and Dugan (CD) are obtained from an impact parameter method[4] by considering only the long-range polarization interaction, neglecting the true elastic scatterings, and assuming the excitation collision to be elastic ($\Delta k^2 = 0$). And in addition, both Smith and Callaway and Dugan have multiplied their cross sections by the ratio of the final and initial relative velocities to take approximate account of the inelastic effects.

Figure 11. The partial elastic cross sections (a_0^2) for even (+) and odd (-) parity scattering channels, $Q_{3/2,1/2}$ (J^+) and $Q_{3/2,1/2}$ (J^-), are plotted vs. J for the incident energy $k_0^2 = 1.255$ (.01 ev).

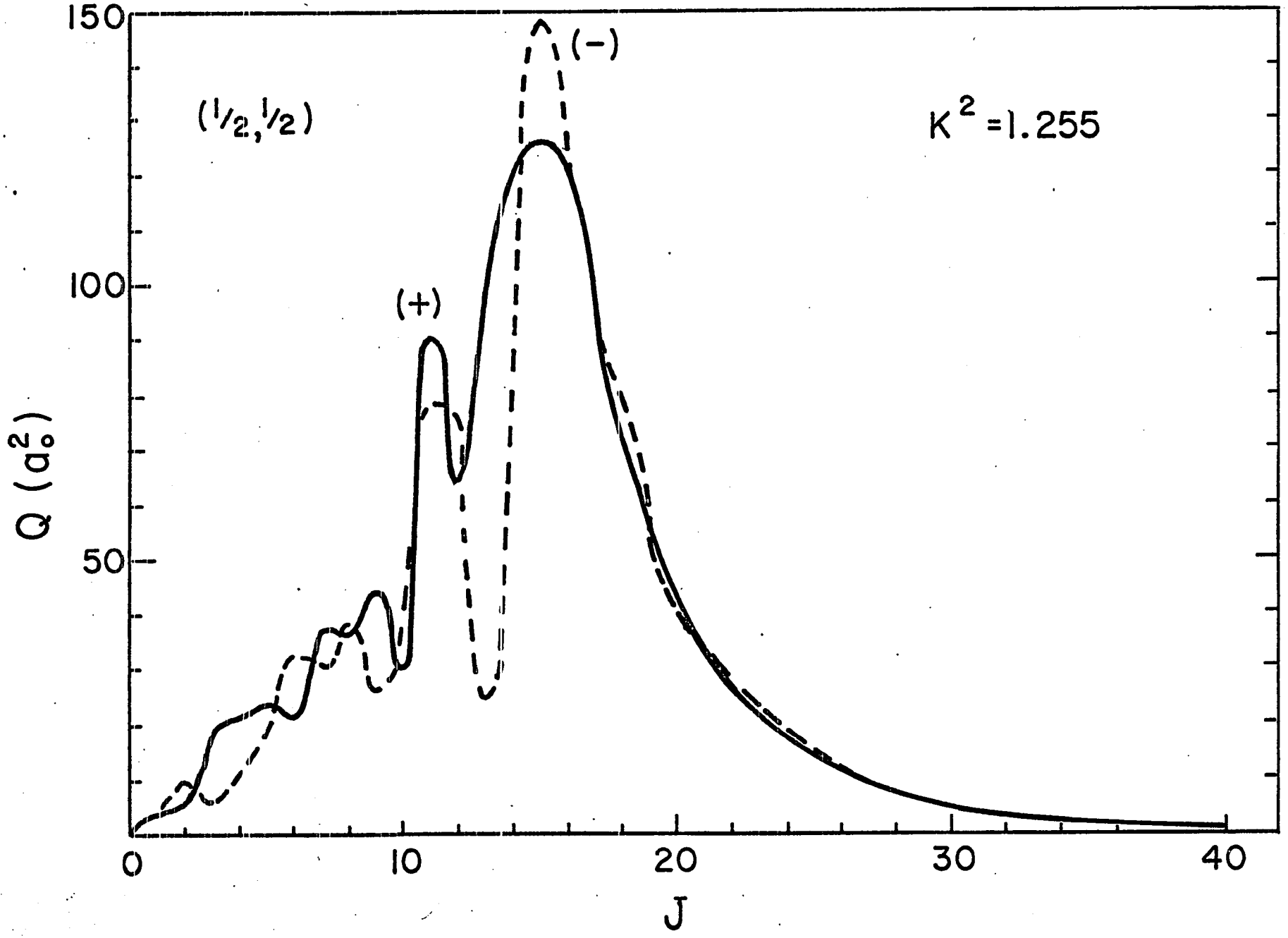
150
100
50
0
10
20
30
40
Q (a_o^2)
J
(1/2, 1/2)
K^2 = 1.255
(+)
(−)

Figure 12. Comparison of the total excitation cross section $Q_{3/2,1/2}$ calculated in this paper (W) with the results of Smith (S), Ref. 7, and Callaway and Dugan (CD), Ref. 6.

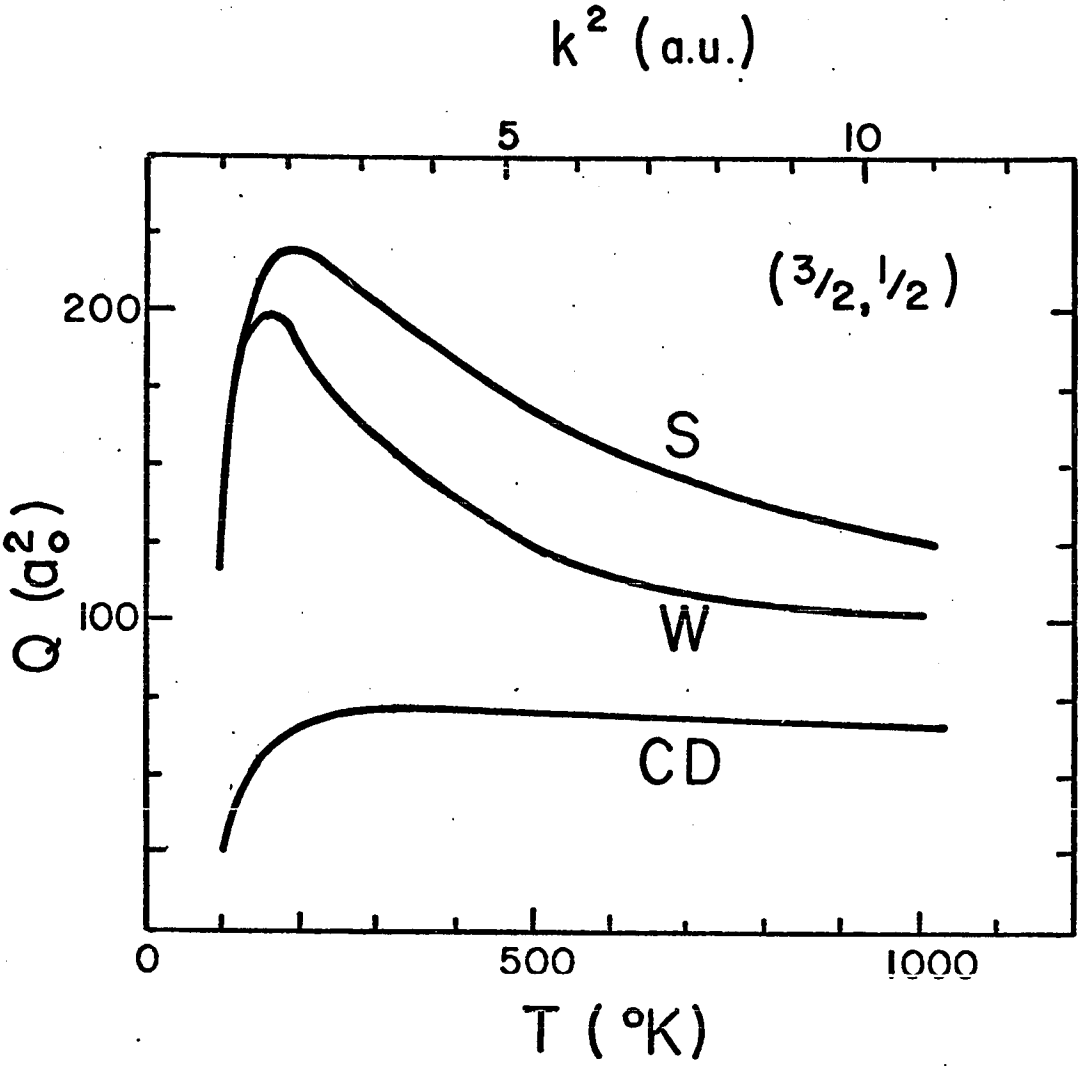
k² (a.u.)
5
10
200
100
Q (a₀²)
(3/2, 1/2)
S
W
CD
0
500
1000
T (°K)

In an attempt to understand the differences among these cross section calculations we first repeated our computations at $k_o^2 = 10.67$ for several even parity channels, including only the (short-range) spin-change coupling terms. In Figure 13 these results (SC) are shown in comparison with results taken from TABLE IV-9, which include both rotational and spin-change coupling terms (RSC). At least at this energy it is apparent that in our close-coupling formulation,

1. the spin-change coupling is much more important than the rotational coupling, and
2. the two coupling mechanisms tend to unpredictably interfere with each other.

We have also recomputed the total excitation cross section at $k_o^2 = 10.67$, neglecting the rotational coupling ($W_2 = 0$) and assuming the collision to be elastic ($\Delta k^2 = 0$). The result,

$$Q_{3/2,1/2}(W_2=0;\ \Delta k^2=0) = 96.64\ a_o^2 ,$$

differs by only 6 percent from the value reported in TABLE IV-2 (and is about 18 percent lower than that calculated by Smith). Thus, at $k_o^2 = 10.67$ the approximations $W_2 = 0$ and $\Delta k^2 = 0$, inherent in Smith's calculation of the C^+ - H excitation cross section, do not significantly change the results of our close coupling calculations. Of course, at lower energies the approximation $\Delta k^2 = 0$ becomes worse. And further, as k_o^2 decreases, we expect the relative importance of the rotational coupling to increase: since fewer scattering

Figure 13. Comparison of the partial excitation cross sections $Q_{3/2,1/2}$ (J^+) for $k_o^2 = 10.67$ computed including both rotational and spin-change coupling (RSC) terms with those computed including only spin-change coupling (SC) terms.

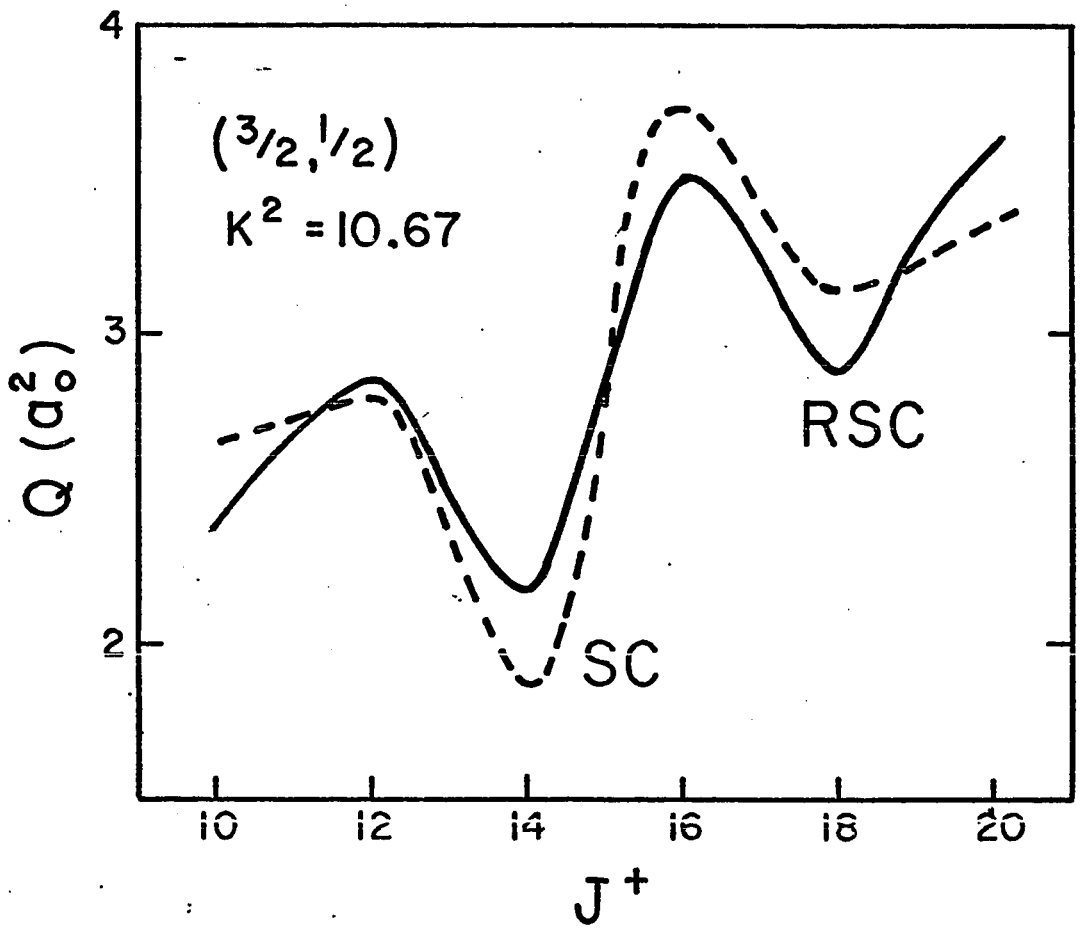
4
3
2
$(^3/_2,^1/_2)$
$K^2 = 10.67$
$Q\ (a_o^2)$
RSC
SC
10
12
14
16
18
20
J^+

channels have classical turning points significantly smaller than the match point R_m, the spin-change coupling process contributes less to the total coupling between the $C^+(^2P)$ levels. We note finally that the orbiting approximation used by Smith assumes that all four CH^+ potentials are dominated by the polarization interaction, having essentially the form $\frac{-\alpha_2}{2R^4}$, so that all four potentials possess deep wells. This, of course, is not the case for the $^3\Sigma^+$ potential (see Figure 2). Moreover, as Smith reported in his investigations[5] of O - H spin-change collisions, the assumption that all four OH potentials are attractive and are dominated by the $\frac{-C}{R^6}$ van der Waals term provides an upper limit at low energies to the O - H excitation cross sections. Evidently this is also true for the C^+ - H excitation cross section.

In addition to the above-mentioned computations, we calculated the excitation cross section for $k_0^2 = 10.67$ after omitting the spin-change coupling terms. As in our full calculations, at small R the spherical term W_0 is transformed to the admixture of CH^+ potential energy curves

$$W_0(R) \xrightarrow[\text{[small R]}]{} \sum_{\Lambda S} P^J_{\Lambda S}(jlj;jlj)\, V_{\Lambda S}(R) \qquad (4.3)$$

The result we obtained was

$$Q_{3/2,1/2}\,(\text{rotational coupling only}) = 3.13\, a_0^2,$$

more than an order of magnitude smaller than the value given by Callaway and Dugan.

It is difficult to give specific reasons for this large discrepency, but one point in particular should be made. In the impact-parameter approximation employed by Callaway and Dugan, the interaction potential actually used in the cross section calculation is just the non-spherical part of the long-range interaction potential, $W_2(R)$. The spherical part $W_0(R)$, which does not couple the $C^+(^2P)$ fine-structure levels but which dominates the trajectories of the atoms at large separations, is neglected. We do not pursue this point further, but it would be interesting to modify the coupled scattering equations by putting $W_0 = 0$ and then calculate the excitation cross section.

In the next section we discuss the sensitivity of our results to several of the parameters and approximations introduced into our close coupling treatment of the C^+ - H scattering problem.

B. Sensitivity of the Results

Because of the numerous approximations made in the development of the scattering equations, and the difficulties associated with the numerical solution of these equations, several input parameters were varied to indicate the sensitivity of our results to specific choices of these parameters. The results discussed below indicate to some extent the uncertainty in the C^+ - H cross sections due to computational techniques and interaction potentials used in our close coupling calculations.

We note first that a general check of the accuracy of the numerical integrations is provided by the symmetry of the computed $\mathbf{R}$ - matrices. A direct consequence of this symmetry is the principle of detailed balance,[28]

$$\frac{Q_{ij}}{\omega_i k_i^2} = \frac{Q_{ji}}{\omega_j k_j^2} \quad , \tag{4.4}$$

where $\omega_j = 2j+1$ is the statistical weight of level (j). We show in TABLE IV-10 the ratios $(Q_{1/2,3/2} / Q_{3/2,1/2})$ predicted by Equation (4.4) and calculated from the results given in TABLE IV-9. The agreement is quite good considering the large number (~2000) of integration steps and accompanying inversions of 6 x 6 matrices involved.

We emphasize, however, that $\mathbf{R}$ -matrix symmetry is only a

TABLE IV-10. $\mathbb{R}$ -matrix symmetry as indicated by the principle of detailed balance(DB), and as computed from the numerical results (N).

$k^2_{J=1/2}$	$(Q_{1/2,3/2}/Q_{3/2,1/2})_{DB}$	$(Q_{1/2,3/2}/Q_{3/2,1/2})_{N}$
1.255	2.424	2.400
1.569	1.369	1.369
1.882	1.062	1.059
2.196	.9150	.9152
3.451	.7029	.7038
6.275	.5943	.5945
10.67	.5515	.5518

measure of the numerical accuracy of the solutions f_{ij} ; it does not provide a check on the correctness of the cross section calculations.

The single factor most strongly affecting the $\mathbb{R}$ -matrix symmetry is the starting points of the numerical integrations. We mentioned earlier the problem of linear dependence among the solutions; if solutions become linearly dependent the $\mathbb{R}$ -matrix becomes asymmetric. To illustrate this point we give in TABLE IV-11 results of starting the numerical integrations with USTART = 50 and USTART = 10, for the case $k_b^2 = 1.255$, $J^\pi = 1, 3, 5, 7, 9$. Listed are the magnitudes of the average deviation of the $\mathbb{R}$ -matrix elements from perfect symmetry,

$$\delta = \frac{1}{N}\left[\sum_{i>j}^{N} \left|1 - (R_{ij}/R_{ji})\right|\right], \qquad (4.5)$$

and the excitation cross sections $Q_{3/2,1/2}$.

As J increases we observe that smaller values of USTART must be used to maintain good symmetry but also that the cross sections become less sensitive to the specific value of USTART. These points are substantiated by the information given in TABLE IV-12. For the case $k_b^2 = 2.510$, $J^\pi = 20$, the cross sections $Q_{1/2,1/2}$, $Q_{1/2,3/2}$, $Q_{3/2,3/2}$ are listed for the four values USTART = 10, 25, 50, 100. For the three larger values of USTART the -matrix is very asymmetric,

TABLE IV-11. Dependence of R -matrix symmetry and excitation cross sections with respect to USTART. $k_e^2 = 1.255$.

J^+	USTART = 50		USTART = 10	
	δ	$(3/2, 1/2)$	δ	$(3/2, 1/2)$
1	.0012	3.217	.0006	2.271
3	.0296	3.572	.0012	4.635
5	.0172	6.868	.0018	7.678
7	.0470	11.84	.0072	10.92
9	.2912	14.28	.0076	15.17

TABLE IV-12. Dependence of the C^+ - H Cross sections with respect to USTART. $J^+ = 20$, $k_e^2 = 2.510$.

USTART	$(1/2, 1/2)$	$(1/2, 3/2)$	$(3/2, 3/2)$
10	77.25	.00114	55.68
25	76.85	.00115	55.72
50	77.56	.00113	57.31
100	77.54	.00114	57.22

$\delta \gtrsim 10^3$, because some of the solutions - all corresponding to the excitation process $C^+(^2P_{1/2}) \Rightarrow C^+(^2P_{3/2})$ - become swamped by the positive exponential terms previously mentioned (c.f. Equation 3.15).

After extensive testing of the $\mathbb{R}$-matrix symmetry for various circumstances we picked the values of USTART = 10, 25 and 50 for certain ranges of J and k_o^2. The specific choices used to obtain the results of the preceding section are

USTART = 50: $J \leq 8$, all k_o^2,
$J > 8$, $k_o^2 > 10$;

USTART = 25: $J > 8$, $5 > k_o^2 \geq 10$;

USTART = 10: $J > 8$, $k_o^2 \leq 5$.

These choices yield symmetric $\mathbb{R}$-matrices, and from data such as given in TABLES IV.11 and IV.12 we estimate that this procedure introduces errors in the total cross sections of less than 10%.

We have also investigated the sensitivity of our results to a particular choice of the point R_m at which the molecular potential energy curves are matched. All of our results in the preceding section were computed with $R_m = 6.0$. At $k_o^2 = 2.196$, near the excitation cross section maximum, our computations were repeated for $J^\pm = 0(2)22$ with the match point $R_m = 8.0$. Again a linear fit was provided for each V_{AS} between $R = 5.0$ and $R = R_m$.

For $J^\pm \geq 18$ the results are identical, indicating that the numerical integrations for these channels are started near or beyond $R_m = 8.0$.

The total cross sections for $k_o^2 = 2.196$ obtained with $R_m = 8.0$ are

$$Q_{1/2,1/2} = 1970.\ a_o^2,$$

$$Q_{1/2,3/2} = 178.4\ a_o^2,$$

$$Q_{3/2,1/2} = 194.9\ a_o^2,$$

$$Q_{3/2,3/2} = 2759.\ a_o^2,$$

Comparing these values with those given in TABLE IV-9 we see that the differences are of the order of 10 percent.

These small differences provide a posteriori justification for our matching the CH^+ potential energy curves to the long-range potential $W_o(R)$ at some intermediate value of the internuclear separation. We should also add that there seems to be little reason to extend the match point beyond $R_m = 8$ since it is evident from TABLE III-1 that there are only negligible changes in the CH^+ curves for $R > 8$.

Our three other investigations regarding the sensitivity of the results given in TABLES IV-3 to IV-9 involve changes in the interaction potentials. The calculations discussed below were done for $k_o^2 = 2.196$.

Now the second order interaction energy ε_2 for C^+ and H atoms at large separations is given by [29]

$$\varepsilon_2 = \sum_{\alpha \neq o} \sum_{\beta \neq o} \frac{|\langle \psi_o^{C^+} \psi_o^H | W | \psi_\alpha^{C^+} \psi_\beta^H \rangle|^2}{(E_\alpha^{C^+} - E_o^{C^+}) + (E_\beta^H - E_o^H)}, \qquad (4.6)$$

where S indicates both a summation over discrete states and an integration over continuum states. We see that averaging $W(\vec{R},\vec{r})$ with respect to the $C^+(2p)$ orbital and orientations $\hat{R}$, denoted $\langle W \rangle$ does not yield this expression (4.6): we have neglected the C^+ states $\alpha \neq 0$ that correspond to closed channels in our scattering problem. Consequently we might expect the energy term $(E_\alpha^{C^+} - E_0^{C^+})$, which is approximately the same size as the term $(E_\beta^H - E_0^H)$ to decrease $\langle W \rangle$ by some 50 percent.

We recomputed the C^+ - H cross section (for $k_0^2 = 2.196$) decreasing for simplicity, only W_2 by one-half. Since the correct asymptotic form of ε_2 is $\sim \frac{-\alpha_2}{2R^4}$, this modification is not unreasonable. The elastic cross sections are changed by less than 5 percent and the excitation cross section is increased by less than 1 percent. This reaffirms our earlier conclusion that the long-range interaction does not affect the scattering cross sections significantly.

Further, increasing the value of the long-range cut-off parameter ρ_2 [c.f. Equation (3.3)] from $6a_0$ to $10a_0$ increases the excitation cross section for the sample case $k_0^2 = 2.196$, $J^+ = 10$ by less than one-half percent, indicating that our results are not sensitive to reasonable variations of ρ_2 either.

And finally, to measure the sensitivity of our results to the precise shape of the (only) repulsive potential curve $^3\Sigma^+$, we decreased $W(^3\Sigma^+)$ by one-half for all $R < 5$. The resulting total cross sections

(again for $k_0^2 = 2.196$),

$$Q_{1/2,\,1/2} = 2041.\ a_0^2,$$

$$Q_{1/2,\,3/2} = 159.0\ a_0^2,$$

$$Q_{3/2,\,1/2} = 173.8\ a_0^2,$$

$$Q_{3/2,\,3/2} = 2602.\ a_0^2,$$

differ by less than 6 percent from those listed in TABLE IV-6; moreover, only partial cross sections $Q(J)$ for $J^2 \leq 16$ differ from those listed in that table.

C. Cooling of Interstellar Hydrogen

As we mentioned in the INTRODUCTION the principal application of this investigation is astrophysical in nature. Collisions of slow hydrogen atoms with the positive ions C^+ and Si^+ and with neutral oxygen atoms are thought to be important cooling mechanisms for interstellar hydrogen clouds (HI regions). In this brief section we discuss only the concepts essential to the calculation of cooling rates due to C^+ - H excitation scattering.

If the radiative lifetime of an excited $C^+(^2P_{3/2})$ ion is significantly shorter than the time between $C^+(^2P_{3/2})$ - H collisions, then excited carbon ions will lose energy almost exclusively by radiative decay. Assuming the density of an interstellar cloud to be 10 hydrogen atoms/cm^3 and the n(H)/n(C+) number density ratio to be 10^4 (c.f. Gould and Salpeter [30]), at a temperature of 125 °K the time between C^+ - H de-excitation collisions is approximately

$$\tau_c = \left[n(H)\, Q_{1/2,3/2}\, v_0 \right]^{-1} \simeq 1 \times 10^8 \text{ sec}, \qquad (4.7)$$

where the initial relative velocity $v_0 = (2 k_B T/\mu)^{1/2}$. The probability of the forbidden $C^+(^2P_{3/2}) \Rightarrow C^+(^2P_{1/2})$ transition, as calculated by Naqui [31] is $A = 2.4 \times 10^{-6}$ sec^{-1}, and so the radiative lifetime of $C^+(^2P_{3/2})$

is

$$\tau_r = 1/A \simeq 4 \times 10^5 \text{ sec.} \qquad (4.8)$$

Comparing these two lifetimes we see that most $C^+(^2P_{3/2})$ ions de-excite radiatively.

Now if the interstellar medium does not absorb this radiation the gas is effectively cooled at a rate

$$\Lambda = (\Delta E)\, n(H) n(C^+) \langle Q_{3/2,1/2}\, v_0 \rangle , \qquad (4.9)$$

where ΔE is the excitation energy of the $C^+(^2P_{3/2})$ level and the integral

$$\langle Q_{3/2,1/2}\, v_0 \rangle = \int dv_0 \left[P(v_0)\, v_0\, Q_{3/2,1/2}(v_0) \right] \qquad (4.10)$$

is a reaction rate averaged with respect to the distribution of relative initial velocities $P(v_0)$.

We obtained a polynomial fit to the total cross section $Q_{3/2,1/2}(v_0)$ and then taking $P(v_0)$ to be a Maxwellian distribution,[5,6] computed the cooling rates Λ (C^+ - H) given in TABLE IV-13. Approximate cooling rates Λ (O - H), estimated from Smith's results[5] with $n(H)/n(O) = 2 \times 10^3$, are also listed in TABLE IV-13.

TABLE IV-13. Rate of cooling of interstellar matter by C^+ - H and O - H fine-structure de-excitation. [$n(H) = 2 \times 10^3$ $n(O) = 10^4$ $n(C^+) = 10$ cm^{-3}].

T(°K)	$\Lambda[C^+-H]$ $\left(\frac{erg}{cm^3\ sec}\right)$	$\Lambda[O-H]$ $\left(\frac{erg}{cm^3\ sec}\right)$
100	6.53×10^{-26}	1.8×10^{-25}
125	7.78×10^{-26}	3.2×10^{-25}
150	8.74×10^{-26}	4.0×10^{-25}
200	1.01×10^{-25}	5.0×10^{-25}
300	1.17×10^{-25}	5.6×10^{-25}
500	1.38×10^{-25}	7.9×10^{-25}

We see that at temperatures characteristic of interstellar hydrogen clouds the C^+ - H excitation collisions provide a significant mechanism for cooling these clouds.

D. Concluding Remarks

It is unfortunate that there are no experimental results with which to compare the cross sections we have computed. Stebbings[32] has indicated that at present there is little hope of measuring the C^+ - H excitation cross section even with a merged beam apparatus since the excitation energy (.0079 ev) is so small. The lack of experimental data concerning this and other, similar fine-structure excitation processes in atom-atom collisions, however, emphasizes the need for precise theoretical computations.

There are various ways in which the calculations we have reported may be improved. It would be very desirable to ascertain what effect a transformation similar to (2.44) but R -dependent would have on the cross section calculations. In addition, it would be preferable to devise within the computer code a better method of starting the numerical integrations. This method would determine if a given solution were becoming too large - resulting in linear dependence - and then restart the integration closer to the classical turning point.

It would also be desirable to compute the cross sections for higher center-of-mass energies to determine when, or if, the semi-classical orbiting and impact-parameter approximations give results in agreement with those obtained by a close coupling formalism.

Finally, we mention some related problems of interest: 1) close coupling calculations of the fine-structure excitation scattering of Si^+ and O by H; 2) inclusion of the spin-change mechanism in collisions such as $O(^3P)$ on $O(^3P)$ where a first-order electrostatic interaction exists; and 3) excitation of upper levels of the ground state configuration of various atoms and ions in collisions with slow hydrogen atoms. Reactions in this third category might prove important in the determination of the statistical equilibria of atoms and ions in HI regions with temperatures $\sim 10^4$ °K.

To calculate any of these cross sections within the framework we have presented requires, of course, detailed knowledge of the relevant molecular potential energy curves. It is encouraging to note that suitable theoretical techniques, such as the pseudopotential method,[33] are now being developed for the calculation of such potential curves.

V. ACKNOWLEDGEMENTS

It is a pleasure to acknowledge my research director, Prof. Neal Lane. His advise and enthusiasm have stimulated much of this investigation. I would also like to acknowledge the informative discussions I have had with Profs. Alex Dalgarno and Ron Stebbings.

The numerical computations described herein were performed at the University of Texas at Austin. The research staffs of Profs. Jim Browne and F. A. Matsen were most courteous and helpful during my frequent visits.

Finally (last the best), I want to thank my wife Janet for her encouragement throughout my graduate studies, and for her recent efforts in the preparation of this manuscript.

During the past year I have been the recipient of a Rice University Graduate Fellowship. In addition, this research was supported in part by a grant from the U. S. Atomic Energy Commission.

VI. REFERENCES

1. N. H. Deiter and W. M. Goss, Rev. Mod. Phys., 38, 256 (1966).

2. A. Dalgarno, Rev. Mod. Phys., 39, 850 (1967).

3. A. Dalgarno and M. R. H. Rudge, Ap. J., 140, 800 (1964).

4. J. Callaway and E. Bauer, Phys. Rev., 140, A1072 (1965).

5. F. J. Smith, Plan. Spa. Sci., 14, 937 (1966).

6. J. Callaway and A. F. Dugan, Phys. Rev., 163, 162 (1967).

7. F. J. Smith, Mon. Not. Roy. Ast. Soc., 140, 341 (1968).

8. D. C. S. Allison and P. G. Burke, Proc. Phys. Soc. (London), Ser. 2, B2, 941 (1969).

9. C. E. Moore, Atomic Energy Levels, I, (1949).

10. A. Dalgarno, Proc. Roy. Soc. (London), A262, 132 (1961).

11. A. M. Arthurs and A. Dalgarno, Proc. Roy. Soc. (London), A256, 540 (1960).

12. M. Born and J. R. Oppenheimer, Ann. d. Phys., 84, 457 (1927).

13. N. F. Mott and H. S. W. Massey, The Theory of Atomic Collisions, (1965).

14. N. F. Lane and S. Geltman, Phys. Rev., 160, 53 (1967).

15. J. N. Murrell et. al., Proc. Roy. Soc. (London), A284, 566, (1965).

16. L. Castillejo, I. C. Percival, and M. J. Seaton, Proc. Roy. Soc. (London), A254, 259 (1960).

17. M. Rotenberg, et. al., The 3-j and 6-j Symbols, (1959).

18. N. F. Mott and H. S. W. Massey, The Theory of Atomic Collisions, (1965).

19. A. C. Allison and A. Dalgarno, Ap. J., 158, 423 (1969).

20. M. E. Rose, Elementary Theory of Angular Momentum, Chap. IV, (1957).

21. P. Moore, Ph. D Thesis, U. Texas (Austin), unpublished, (1965).

22. J. C. Browne, private communication (1970).

23. P. L. Moore, et. al., J. Chem. Phys., 43, 903 (1965).

24. E. Clementi, I. B. M. J. Res. Devel. (Suppl.), 9 (1965).

25. D. R. Hartree, The Calculation of Atomic Structures, (1957).

26. L. L. Barnes, N. F. Lane, and C. C. Lin, Phys. Rev., 137, A388 (1965).

27. Handbook of Mathematical Functions, ed. by M. Abramowitz and I. A. Stegun, App. Math. Ser. 55 (1964).

28. E. H. S. Burhop, Quantum Theory, Vol. I, ed. D. R. Bates, 370 (1961).

29. A. Dalgarno and W. D. Davison, Advances in Atomic and Molecular Physics, Vol. 2 (1966).

30. R. J. Gould and E. E. Salpeter, Ap. J., 138, 393 (1963).

31. A. M. Naqui, Thesis, Harvard University (1951).

32. R. F. Stebbings, private communication (1970).

33. J. D. Weeks, et. al., Advances in Chemical Physics, XVI, 283 (1969).

34. L. Pauling and E. B. Wilson, Introduction to Quantum Mechanics, (1935).

35. M. E. Rose, J. Math and Phys., 37, 215 (1958).

36. A. Dalgarno, Advances in Physics, 11, 281 (1962).

APPENDIX A

We wish to derive the second order energy correction W for a hydrogen atom perturbed by a carbon ion. The notation is that of Chapter II.

Averaging over the $C^+(1s^2 2s^2)$ core, the effective interaction potential for C^+ and H may be written as

$$\tilde{v} = 2\left(\frac{1}{R} - \frac{1}{r_{a1}}\right) + \left(\frac{1}{r_{12}} - \frac{1}{r_{b2}}\right). \qquad \text{(A. 1)}$$

Using standard perturbation techniques (see, for example, Pauling and Wilson, Chapter VI.) we obtain

$$W = \sum_{\beta \neq 0} \frac{|\langle 0|\tilde{v}|\beta\rangle|^2}{E_0^H - E_\beta^H}, \qquad \text{(A. 2)}$$

where $|\beta\rangle$ is the β th state of hydrogen, with energy E_β^H, and $\sum$ indicates both a summation over discrete states and an integration over continuum states, the initial state $|0\rangle$ being omitted.

To calculate W, following Rose[35] we expand the interparticle distance

$$\frac{1}{r_{ij}} = \sum_{s,t=0}^{\infty} \frac{b_{st}}{R^{s+t+1}} \sum_{\lambda} T_\lambda^{s+t*}(i,j)\, C_\lambda^{s+t}(\hat{R}), \qquad \text{(A. 3)}$$

where $\mathbb{C}^{\ell}_{m}$ is a component of the irreducible spherical tensor $\mathbb{C}^{(\ell)}$, the tensor component

$$T_{\lambda}^{s+t}(i,j) = \sum_{\mu\nu} (s\mu t\nu | s+t,\lambda)\, r_{ai}^{s}\, r_{bj}^{t}\, \mathbb{C}^{s}_{\mu}(\hat{r}_{ai})\, \mathbb{C}^{t}_{\nu}(\hat{r}_{bj}), \quad \text{(A. 4)}$$

and the coefficient

$$b_{st} = (-)^{s} \left[\frac{(2s+2t)!}{(2s)!\,(2t)!} \right]^{1/2}. \quad \text{(A. 5)}$$

With this notation we may write the C^{+} - H interaction as

$$\tilde{w} = 2\left[\frac{1}{R} - \sum_{s,t=0}^{\infty} \delta(s,0) \frac{b_{st}}{R^{s+t+1}} \sum_{\lambda} T_{\lambda}^{s+t\,*}(a,1)\, \mathbb{C}^{s+t}_{\lambda}(\hat{R}) \right] \quad \text{(A. 6)}$$

$$+ \sum_{s,t=0}^{\infty} \frac{b_{st}}{R^{s+t+1}} \sum_{\lambda} \left[T_{\lambda}^{s+t*}(2,1)\, \mathbb{C}^{s+t}_{\lambda}(\hat{R}) - \delta(s,0)\, T_{\lambda}^{s+t*}(b,2)\, \mathbb{C}^{s+t}_{\lambda}(\hat{R}) \right].$$

It is most convenient to choose a coordinate system with the quantization axis along $\vec{R}$, for in this system $\hat{R} = 0$ and (A. 6) can be reduced to the simpler expression

$$\tilde{w} = -2 \sum_{s,t=1}^{\infty} \delta(s,0) \frac{b_{st}}{R^{s+t+1}}\, T_{0}^{s+t\,*}(b,1) \quad \text{(A. 7)}$$

$$+ \sum_{s,t=0}^{\infty} \frac{b_{st}}{R^{s+t+1}} \left[T_{0}^{s+t\,*}(2,1) - \delta(s,0)\, T_{0}^{s+t\,*}(b,2) \right].$$

For the hydrogenic state

$$|\beta\rangle = |nLM\rangle \Rightarrow R_{nL}(r_{b1})\, Y_{LM}(\hat{r}_{b1}) ,$$

a matrix element of (A. 2) may now be calculated,

$$\begin{aligned}
\langle \beta | \tilde{w} | o \rangle &= \langle nLM | \tilde{w} | 100 \rangle \\
&= -2 \sum_{t=1}^{\infty} \frac{b_{ot}}{R^{t+1}}\, \delta(\nu,0) \langle nL | r_{b1}^{t} | 10 \rangle \langle LM | C_{\nu}^{t\,*}(\hat{r}_{b1}) | 00 \rangle \\
&\quad + \sum_{s,t=o}^{\infty} \frac{b_{st}}{R^{s+t+1}} \sum_{\nu} (s,-\nu,t,\nu | s+t,o)\, r_{a2}^{s}\; C_{-\nu}^{s\,*}(\hat{r}_{a2}) \qquad \text{(A. 8)} \\
&\qquad \times \langle nL | r_{b1}^{t} | 10 \rangle \langle LM | C_{\nu}^{t\,*}(\hat{r}_{b1}) | 00 \rangle \\
&\quad + \sum_{t=o}^{\infty} \frac{-b_{ot}}{R^{t+1}} \sum_{\nu} (s,-\nu,t,\nu | s+t,o)\, r_{a2}^{s}\; C_{-\nu}^{s\,*}(\hat{r}_{a2}) \langle nLM | 100 \rangle .
\end{aligned}$$

In (A. 8) the radial and angular integrals are

$$\langle nL | r^{t} | 10 \rangle = \int_{o}^{\infty} dr \left[r^{2} R_{nL}(r)\, r^{t}\, R_{10}(r) \right] , \qquad \text{(A. 9)}$$

and

$$\begin{aligned}
\langle LM | C_{\mu}^{\lambda}(\hat{r}) | 00 \rangle &= \langle LM | C_{\mu}^{\lambda}(\vartheta,\varphi) | 00 \rangle \qquad \text{(A. 10)} \\
&= \int_{0}^{2\pi} d\varphi \int_{0}^{\pi} d\vartheta \left[\sin\vartheta\; Y_{LM}^{*}(\vartheta,\varphi)\, C_{\mu}^{\lambda}(\vartheta,\varphi)\, Y_{00}(\vartheta,\varphi) \right] .
\end{aligned}$$

Because $|\beta\rangle = |100\rangle$ is excluded from the summation (A. 2), the last term of (A. 8) vanishes. Reducing the remaining terms it follows that

$$\langle nLM|\tilde{v}|100\rangle = (-)^M \frac{\langle nL|r_{b1}^L|10\rangle}{(2L+1)^{1/2}}$$

$$\times \sum_{s=0}^{\infty} \frac{b_{sL}}{R^{s+L+1}} [1-2\delta(s,0)] (sML-M|s+L,0) r_{a2}^s \mathbb{C}_M^{s*}(\hat{r}_{a2}). \tag{A. 11}$$

With the above result we may immediately write down the second order energy correction,

$$W = \sum_{(nLM)} \left\{ \frac{\langle nL|r_{b1}^L|10\rangle^2}{(2L+1)(E_1^H - E_n^H)} \right\} \sum_{s,t=0}^{\infty} [1-2\delta(s,0)][1-2\delta(t,0)]$$

$$\times \frac{b_{sL} b_{tL} r^{s+t}}{R^{s+t+2L+2}} \mathbb{C}_M^{s*}(\hat{r}) \mathbb{C}_M^{t}(\hat{r}) (sML-M|s+L,0) \tag{A. 12}$$

$$\times (tML-M|t+L,0),$$

the subscripts on the carbon electron coordinates having been dropped. The bracketed term in (A. 12) is related to the 2^L -pole polarizability of hydrogen,[36]

$$\alpha_{2^L} = \frac{2}{2L+1} \sum_n \frac{\langle nL|r^L|10\rangle^2}{(E_n^H - E_1^H)}, \tag{A. 13}$$

so that expanding (A. 12) through terms of the order R^{-6},

$$W = \frac{-\alpha_2}{2R^4}\left[\sum_{s+t\in 2}[1-2\delta(s,0)][1-2\delta(t,0)]\ \frac{b_{s1}\,b_{t1}\,r^{s+t}}{R^{s+t}}\right.$$

$$\left.\times\sum_{M}(sM1\,-M\,|s+1,0)(tM1\,-M\,|t+1,0)\,C_M^{s*}(\hat{r})\,C_M^{t}(\hat{r})\right] \quad \text{(A. 14)}$$

$$-\frac{\alpha_4}{2R^6} \qquad + \mathcal{O}(R^{-7})\,.$$

Evaluating the coupling coefficients and noting that $[C_0^1(\hat{r})]^2 = \frac{1}{3}[2\,C_0^2(\hat{r})+1]$, the second order energy correction

$$W = \frac{-\alpha_2}{2R^4}\left\{1-4\frac{r}{R}C_0^1(\hat{r})+\frac{r^2}{R^2}[2-4\,C_0^2(\hat{r})]\right\}-\frac{\alpha_4}{2R^6}\,. \quad \text{(A. 15)}$$

Since $C_0^\lambda(\vartheta,\varphi)$ is the Legendre polynomial $P_\lambda(\cos\vartheta)$, we see that the angular dependence of W is determined only by the angle between the $C^+(2p)$ electron coordinate r and the internuclear axis R . We can express W in the CM system where $\vec{R}$ and $\vec{r}$ have spherical polar angles $\hat{R}$ and $\hat{r}$ by rotating the quantity (A. 15) through the angles $\hat{R}$. By straight foreward application of the rotation operators,[20] each angular term transforms as

$$\sum_{\mu} D^{\lambda}_{\mu 0}(\varphi_R,\vartheta_R,0)\,C_0^\lambda(\vartheta_r,\varphi_r)\,. \quad \text{(A. 16)}$$

But $D^{\lambda}_{\mu 0}(\varphi_R, \vartheta_R, 0)$ is just $C^{\lambda *}_{\mu}(\vartheta_R, \varphi_R)$, so that upon using the familiar spherical harmonic addition theorem we find

$$W = -\frac{\alpha_2}{2R^4}\left\{1 - 4\frac{r}{R}P_1(\vec{r}\cdot\vec{R}) + \frac{r^2}{R^2}\left[2 - 4P_2(\vec{r}\cdot\vec{R})\right]\right\} - \frac{\alpha_4}{2R^6}, \tag{A.17}$$

where the argument of the Legendre polynomials is the cosine of the angle between $\vec{r}$ and $\vec{R}$.

APPENDIX B

In this section we reduce the coupling matrix element

$\langle \mathcal{Y}^{JM}_{jl} | W | \mathcal{Y}^{J'M'}_{j'l'} \rangle$, where $\mathcal{Y}^{JM}_{jl}$ is given by (2.14),

$$\mathcal{Y}^{JM}_{jl} = \sum_{m_j, m_l} (j m_j l m_l | J M) \phi^{ct}_{j m_j}(\vec{r}) Y_{l m_l}(\hat{R}) . \qquad (B.1)$$

and the interaction potential W is given by (2.36),

$$W(\vec{R}, \vec{r}) = \sum_{\lambda\mu} W_\lambda(R, r) \left(\frac{2\lambda+1}{4\pi}\right) Y^*_{\lambda\mu}(\hat{R}) Y_{\lambda\mu}(\hat{r}) . \qquad (B.2)$$

We first introduce the more symmetrical coupling coefficient, the 3-j symbol of Wigner,[17]

$$\begin{pmatrix} j_1 & j_2 & j_3 \\ m_1 & m_2 & -m_3 \end{pmatrix} = (-)^{-j_1+j_2-m_3} (2j_3+1)^{-1/2} (j_1 m_1 j_2 m_2 | j_3 -m_3) . \qquad (B.3)$$

and the spherical tensor component,

$$C^\lambda_\mu(\hat{x}) = \left(\frac{2\lambda+1}{4\pi}\right)^{1/2} Y_{\lambda\mu}(\hat{x}) . \qquad (B.4)$$

Then it follows that

$$\langle y_{jl}^{jm} | w | y_{j'l'}^{j'm'} \rangle$$

$$= \sum_{\substack{m_j m_l \\ m_j' m_l' \\ \lambda \mu}} (-)^S \left[(2j+1)(2j'+1)(2l+1)(2l'+1)\right]^{1/2} W_\lambda(R)$$

$$\times \begin{pmatrix} 1 & 1/2 & j \\ m & m_s & -m_j \end{pmatrix} \begin{pmatrix} 1 & 1/2 & j' \\ m' & m_s' & -m_j' \end{pmatrix} \begin{pmatrix} j & l & j \\ m_j & m_l & -m \end{pmatrix} \qquad \text{(B. 5)}$$

$$\times \begin{pmatrix} j' & l' & j' \\ m_j' & m_l' & -m' \end{pmatrix} \delta(m_s, m_s') \langle l m_l | C_\mu^{\lambda *} | l' m_l' \rangle$$

$$\times \langle 1 m | C_\mu^\lambda | 1 m' \rangle ,$$

where

$$S = -(1 + m_j + m_j' + l + j' - l - l' + m + m') \qquad \text{(B. 6)}$$

and $W_\lambda(R)$ is $W_\lambda(R,r)$ averaged with respect to the $C^+(2p)$ orbital.

The angular integrals are evaluated to be

$$\langle l m_l | C_\mu^{\lambda *} | l' m_l' \rangle = (-)^{-\mu - m_l} \begin{pmatrix} l & \lambda & l' \\ 0 & 0 & 0 \end{pmatrix} \begin{pmatrix} l & \lambda & l' \\ -m_l & -\mu & m_l' \end{pmatrix} \qquad \text{(B. 7)}$$

$$\times \left[(2l+1)(2l'+1)\right]^{1/2} ,$$

and

$$\langle 1 m | C_\mu^\lambda | 1 m' \rangle = (-)^m 3 \begin{pmatrix} 1 & \lambda & 1 \\ 0 & 0 & 0 \end{pmatrix} \begin{pmatrix} 1 & \lambda & 1 \\ -m & \mu & m' \end{pmatrix} . \qquad \text{(B. 8)}$$

Upon substituting (B. 7) and (B. 8) into (B. 5) we find

$$\langle \mathcal{Y}_{jl}^{gm} | w | \mathcal{Y}_{j'l'}^{g'm'} \rangle$$

$$= (-)^{l+l'-j-j'-m-m'-1} \; 3\left[(2l+1)(2l'+1)(2j+1)(2j'+1)\right.$$

$$\left.\times(2g+1)(2g'+1)\right]^{1/2} \sum_{\lambda} W_{\lambda}(R) \begin{pmatrix} 1 & \lambda & 1 \\ 0 & 0 & 0 \end{pmatrix}\begin{pmatrix} l & \lambda & l' \\ 0 & 0 & 0 \end{pmatrix}$$

$$\times \sum_{\substack{m_l m_l' \\ m_g m_g' \\ m\, m' \\ m_\lambda \mu}} (-)^{-m_g - m_g' - \mu - m_l - m} \begin{pmatrix} 1 & \tfrac{1}{2} & j \\ m & m_\lambda & -m_g \end{pmatrix}\begin{pmatrix} 1 & \tfrac{1}{2} & j' \\ m' & m_\lambda & -m_g' \end{pmatrix} \quad \text{(B. 9)}$$

$$\times \begin{pmatrix} j & l & g \\ m_g & m_l & -m \end{pmatrix}\begin{pmatrix} j' & l' & g' \\ m_g' & m_l' & -m' \end{pmatrix}\begin{pmatrix} l & \lambda & l' \\ -m_l & -\mu & m_l' \end{pmatrix}$$

$$\times \begin{pmatrix} 1 & \lambda & 1 \\ -m & \mu & m' \end{pmatrix}.$$

We now make use of a relationship involving the 6-j symbol of Wigner, $\begin{Bmatrix} j_1 & j_2 & j_3 \\ j_4 & j_5 & j_6 \end{Bmatrix}$, namely,

$$\begin{pmatrix} j_1 & j_2 & j_3 \\ m_1 & m_2 & m_3 \end{pmatrix}\begin{Bmatrix} j_1 & j_2 & j_3 \\ l_1 & l_2 & l_3 \end{Bmatrix}$$

$$= \sum_{\text{all } \bar{n}} (-)^{l_1+l_2+l_3+\bar{n}_1+\bar{n}_2+\bar{n}_3} \begin{pmatrix} j_1 & l_2 & l_3 \\ \bar{m}_1 & \bar{n}_2 & -\bar{n}_3 \end{pmatrix}\begin{pmatrix} l_1 & j_2 & l_3 \\ -\bar{n}_1 & \bar{m}_2 & \bar{n}_3 \end{pmatrix}\begin{pmatrix} l_1 & l_2 & j_3 \\ \bar{n}_1 & -\bar{n}_2 & \bar{m}_3 \end{pmatrix}. \quad \text{(B. 10)}$$

In (B. 9), summing first over (m , m' , m_s), and then over (μ , m_ℓ , m_j), we obtain

$$\langle y^{qm}_{j\ell} | w | y^{q'm'}_{j'\ell'} \rangle$$

$$= (-)^{-m-m'-3/2} 3 [(2j+1)(2j'+1)(2\ell+1)(2\ell'+1)(2q+1)$$

$$\times (2q'+1)]^{1/2} \sum_\lambda (-)^\lambda W_\lambda(R) \quad (-)^{-j'+\ell} \qquad \text{(B. 11)}$$

$$\times \begin{pmatrix} 1 & \lambda & 1 \\ 0 & 0 & 0 \end{pmatrix} \begin{pmatrix} \ell & \lambda & \ell' \\ 0 & 0 & 0 \end{pmatrix} \begin{Bmatrix} j & j' & \lambda \\ 1 & 1 & 1/2 \end{Bmatrix} \begin{Bmatrix} \ell' & j' & q \\ j & \ell & \lambda \end{Bmatrix}$$

$$\times \sum_{m_\ell m_j} \begin{pmatrix} \ell' & q & j' \\ m_\ell & -m & m_j \end{pmatrix} \begin{pmatrix} j' & j & \ell' \\ m_j & -m' & m_\ell \end{pmatrix}$$

which reduces easily to the result

$$\langle y^{qm}_{j\ell} | w | y^{q'm'}_{j'\ell'} \rangle$$

$$= \delta(q,q') \, \delta(m,m') \, 3 [(2\ell+1)(2\ell'+1)(2j+1)(2j'+1)]^{1/2} \qquad \text{(B. 12)}$$

$$\times \sum_\lambda (-)^{q-1/2-\lambda} W_\lambda(R) \begin{pmatrix} 1 & \lambda & 1 \\ 0 & 0 & 0 \end{pmatrix} \begin{pmatrix} \ell & \lambda & \ell' \\ 0 & 0 & 0 \end{pmatrix} \begin{Bmatrix} j & j' & \lambda \\ 1 & 1 & 1/2 \end{Bmatrix} \begin{Bmatrix} j & j' & \lambda \\ \ell' & \ell & q \end{Bmatrix},$$

by use of the orthogonality relation

$$\sum_{m_1 m_2} \begin{pmatrix} j_1 & j_2 & j_3 \\ m_1 & m_2 & m_3 \end{pmatrix} \begin{pmatrix} j_1 & j_2 & j_3' \\ m_1 & m_2 & m_3' \end{pmatrix} = \frac{\delta(j_3, j_3')\,\delta(m_3, m_3')}{(2j_3+1)} \,. \tag{B. 13}$$

We note that since

$$\begin{pmatrix} j_1 & j_2 & j_3 \\ 0 & 0 & 0 \end{pmatrix} = 0 \qquad \text{unless } (j_1 + j_2 + j_3) \text{ = even integer}$$

only even values of λ contribute non-vanishing coupling matrix elements.

APPENDIX C

In this section we reduce the spin-change coupling matrix elements appearing in Equation (2.44). We define

$$\langle \Gamma^{JM}_{j\ell g} \mid v \mid \Gamma^{JM}_{j'\ell'g'} \rangle = \sum_{\Lambda S} v_{\Lambda S}(R)\, P^{J}_{\Lambda S}(j\ell g; j'\ell' g') , \tag{C.1}$$

where

$$\begin{aligned} P^{J}_{\Lambda S}(j\ell g; j'\ell' g') &= \sum (j m_j \ell m_\ell \mid g m)(j' m_{j'} \ell' m_{\ell'} \mid g' m') \\ &\times (g m \tfrac{1}{2}\sigma \mid JM)(g' m' \tfrac{1}{2}\sigma' \mid JM) \\ &\times \langle j \tilde{m}_j \tilde{\sigma} \mid \Lambda S M_S \rangle \langle \Lambda S M_S \mid j' \tilde{m}_{j'} \tilde{\sigma}' \rangle \\ &\times \langle Y_{\ell m_\ell} D^{1}_{\tilde{m}_j m_j} D^{1/2}_{\tilde{\sigma}\sigma} \mid Y_{\ell' m_{\ell'}} D^{1'}_{\tilde{m}_{j'} m_{j'}} D^{1/2}_{\tilde{\sigma}'\sigma'} \rangle , \end{aligned} \tag{C.2}$$

and where the summation is over the quantities

$$\{ m\, m'\, m_\ell\, m_{\ell'}\, m_j\, m_{j'}\, \sigma\, \sigma'\, \tilde{m}_j\, \tilde{m}_{j'}\, \tilde{\sigma}\, \tilde{\sigma}'\, M_S \} .$$

We first evaluate the integration over the orientation angles $\hat{R}$. From Rose,[20] we have

$$Y_{\lambda\mu}(\hat{R}) = \left(\frac{2\lambda+1}{4\pi}\right)^{1/2} D^{*\lambda}_{\mu 0}(\varphi_R, \vartheta_R, 0) \equiv \left(\frac{2\lambda+1}{4\pi}\right)^{1/2} D^{*\lambda}_{\mu 0}(\hat{R}), \quad \text{(C. 3)}$$

$D^{\lambda}_{\mu\nu}$ being an element of the rotation matrix, and also

$$D^{\lambda}_{m\mu}(\hat{R})\, D^{\lambda'}_{m'\mu'}(\hat{R}) = \sum_{\ell n \nu} (2\ell+1) \begin{pmatrix} \lambda & \lambda' & \ell \\ m & m' & n \end{pmatrix} \begin{pmatrix} \lambda & \lambda' & \ell \\ \mu & \mu' & \nu \end{pmatrix} D^{*\ell}_{n\nu}(\hat{R}). \quad \text{(C. 4)}$$

Applying the relation (C. 4) three times we calculate

$$\begin{aligned}
&\langle Y_{\ell m_\ell}\, D^{j}_{\tilde{m}_j m_j}\, D^{1/2}_{\tilde{\sigma}\sigma} \mid Y_{\ell' m'_\ell}\, D^{j'}_{\tilde{m}'_j m'_j}\, D^{1/2}_{\tilde{\sigma}'\sigma'} \rangle \\
&= (-)^{m_\ell} \left[\frac{(2\ell+1)(2\ell'+1)}{(4\pi)^2}\right]^{1/2} \sum_{\begin{Bmatrix} a & \alpha & \tilde{\alpha} \\ b & \beta & \tilde{\beta} \\ c & \gamma & \tilde{\gamma} \end{Bmatrix}} (2a+1)(2b+1)(2c+1)\,(-)^{\tilde{\beta}-\beta} \\
&\quad \times \begin{pmatrix} \ell & \ell' & c \\ 0 & 0 & 0 \end{pmatrix} \begin{pmatrix} j & 1/2 & a \\ \tilde{m}_j & \tilde{\sigma} & \tilde{\alpha} \end{pmatrix} \begin{pmatrix} j & 1/2 & a \\ m_j & \sigma & \alpha \end{pmatrix} \begin{pmatrix} j' & 1/2 & b \\ \tilde{m}'_j & \tilde{\sigma}' & \tilde{\beta} \end{pmatrix} \begin{pmatrix} j' & 1/2 & b \\ m'_j & \sigma' & \beta \end{pmatrix} \\
&\quad \times \begin{pmatrix} \ell & \ell' & c \\ -m_\ell & m'_\ell & \tilde{\gamma} \end{pmatrix} \int d\hat{R} \left[D^{a}_{\tilde{\alpha}\alpha}(\hat{R})\, D^{b}_{\tilde{\beta}\beta}(\hat{R})\, D^{c}_{\tilde{\gamma}0}(\hat{R}) \right] \\
&= (-)^{m_\ell} \left[(2\ell+1)(2\ell'+1)\right]^{1/2} \sum_{\begin{Bmatrix} a & \alpha & \tilde{\alpha} \\ b & \beta & \tilde{\beta} \\ c & \gamma & \tilde{\gamma} \end{Bmatrix}} (2a+1)(2b+1)(2c+1)\,(-)^{\tilde{\beta}-\beta} \\
&\quad \times \begin{pmatrix} \ell & \ell' & c \\ 0 & 0 & 0 \end{pmatrix} \begin{pmatrix} j & 1/2 & a \\ \tilde{m}_j & \tilde{\sigma} & \tilde{\alpha} \end{pmatrix} \begin{pmatrix} j & 1/2 & a \\ m_j & \sigma & \alpha \end{pmatrix} \begin{pmatrix} j' & 1/2 & b \\ \tilde{m}'_j & \tilde{\sigma}' & \tilde{\beta} \end{pmatrix} \\
&\quad \times \begin{pmatrix} j' & 1/2 & b \\ m'_j & \sigma' & \beta \end{pmatrix} \begin{pmatrix} \ell & \ell' & c \\ -m_\ell & m'_\ell & \tilde{\gamma} \end{pmatrix} \begin{pmatrix} a & b & c \\ \tilde{\alpha} & -\tilde{\beta} & \tilde{\gamma} \end{pmatrix} \begin{pmatrix} a & b & c \\ \alpha & -\beta & 0 \end{pmatrix} .
\end{aligned} \quad \text{(C. 5)}$$

Now substituting the result (C.5) into (C.2) and using 3-j symbols throughout we obtain

$$
\begin{aligned}
&P_{\Lambda S}^{J}(j\ell g; j'\ell'g') \\
&= (2J+1)(2S+1)\left[(2j+1)(2j'+1)(2\ell+1)(2\ell'+1)(2g+1)(2g'+1)\right]^{1/2} \\
&\times (-)^{\ell+\ell'-j-j'-g-g'} \sum (-)^{m_\ell+\beta-\tilde{\beta}-\tilde{m}_j-\tilde{m}_j'-\mathcal{M}-\mathcal{M}'}(2a+1)(2b+1) \\
&\times (2c+1)\begin{pmatrix} j & \ell & g \\ m_j & m_\ell & -\mathcal{M}\end{pmatrix}\begin{pmatrix} g & 1/2 & J \\ \mathcal{M} & \sigma & -M\end{pmatrix}\begin{pmatrix} j' & \ell' & g' \\ m_j' & m_\ell' & -\mathcal{M}'\end{pmatrix}\begin{pmatrix} g' & 1/2 & J \\ \mathcal{M}' & \sigma' & -M\end{pmatrix} \\
&\times \begin{pmatrix} 1 & 1/2 & j \\ m & m_a & -m_j\end{pmatrix}\begin{pmatrix} 1 & 1/2 & j' \\ m' & m_a' & -m_j'\end{pmatrix}\begin{pmatrix} 1/2 & 1/2 & S \\ m_a & \tilde{\sigma} & -M_S\end{pmatrix}\begin{pmatrix} 1/2 & 1/2 & S \\ m_a' & \tilde{\sigma}' & -M_S\end{pmatrix} \qquad \text{(C.6)} \\
&\times \begin{pmatrix} \ell & \ell' & c \\ 0 & 0 & 0\end{pmatrix}\begin{pmatrix} \ell & \ell' & c \\ -m_\ell & m_\ell' & \tilde{\gamma}\end{pmatrix}\begin{pmatrix} j & 1/2 & a \\ \tilde{m}_j & \tilde{\sigma} & \tilde{\alpha}\end{pmatrix}\begin{pmatrix} j & 1/2 & a \\ m_j & \sigma & \alpha\end{pmatrix} \\
&\times \begin{pmatrix} j' & 1/2 & b \\ \tilde{m}_j' & \tilde{\sigma}' & \tilde{\beta}\end{pmatrix}\begin{pmatrix} j' & 1/2 & b \\ m_j' & \tilde{\sigma} & \beta\end{pmatrix}\begin{pmatrix} a & b & c \\ \tilde{\alpha} & -\tilde{\beta} & \tilde{\gamma}\end{pmatrix}\begin{pmatrix} a & b & c \\ \alpha & -\beta & 0\end{pmatrix},
\end{aligned}
$$

where the summation is over a, b, and c and all projection quantum numbers

$$\{ m_\ell\, m_\ell'\, m_j\, m_j'\, \sigma\, \sigma'\, \tilde{m}_j\, \tilde{m}_j'\, \tilde{\sigma}\, \tilde{\sigma}'\, M_s \;\; m\, m'\, m_s\, m_s'\, \alpha\, \tilde{\alpha}\, \beta\, \tilde{\beta}\, \tilde{\gamma} \},$$

with the restriction $|m| = \Lambda$. Employing the relation (B.10), summing first over ($\tilde{m}_j'$, σ', $\mathcal{M}'$) and (m_j, σ, $\mathcal{M}$), then over

$(\tilde{m}_j', \tilde{\sigma}', m_s')$ and $(\tilde{m}_j, \tilde{\sigma}, m_s)$, and then over $(M_s, \tilde{\alpha}, \tilde{\beta})$ and (M, α, β), dividing by $(2J+1)$, we may reduce (C.6) to

$$
\begin{aligned}
P^J_{\Lambda S}(jlq; j'l'q') &= (2S+1)\left[(2j+1)(2j'+1)(2l+1)(2l'+1)(2q+1)(2q'+1)\right]^{1/2} \\
&\times (-)^{1-J-S-q-q'} \sum_{m_l m_l'} \sum_{|m|=\Lambda} (-)^m \sum_{(abc\tilde{\gamma})} (2a+1)(2b+1)(2c+1) \qquad \text{(C.7)} \\
&\times \begin{pmatrix} l & l' & c \\ 0 & 0 & 0 \end{pmatrix} \begin{pmatrix} l & l' & c \\ -m_l & m_l' & \tilde{\gamma} \end{pmatrix} \begin{pmatrix} 1 & 1 & c \\ -m_l' & m_l & \tilde{\gamma} \end{pmatrix} \begin{pmatrix} l & l' & c \\ -m_l & m_l' & 0 \end{pmatrix} \begin{Bmatrix} 1 & 1 & c \\ a & b & S \end{Bmatrix} \\
&\times \begin{Bmatrix} J & l & a \\ j & 1/2 & q \end{Bmatrix} \begin{Bmatrix} J & l' & b \\ j' & 1/2 & q' \end{Bmatrix} \begin{Bmatrix} 1 & a & S \\ 1/2 & 1/2 & j \end{Bmatrix} \begin{Bmatrix} 1 & b & S \\ 1/2 & 1/2 & j' \end{Bmatrix} \begin{Bmatrix} l' & l & c \\ a & b & J \end{Bmatrix}.
\end{aligned}
$$

And finally, by employing the orthogonality relation (B.13), we may reduce the spin-change coupling matrix element to the desired form,

$$
\begin{aligned}
P^J_{\Lambda S}(jlq; j'l'q') &= (2S+1)\left[(2j+1)(2j'+1)(2l+1)(2l'+1)(2q+1)(2q'+1)\right]^{1/2} \\
&\times (-)^{1-J-S-q-q'} \sum_{(abc)} (2a+1)(2b+1) \begin{pmatrix} l & l' & c \\ 0 & 0 & 0 \end{pmatrix} \qquad \text{(C.8)} \\
&\times \begin{Bmatrix} J & l & a \\ j & 1/2 & q \end{Bmatrix} \begin{Bmatrix} J & l' & b \\ j' & 1/2 & q' \end{Bmatrix} \begin{Bmatrix} 1 & a & S \\ 1/2 & 1/2 & j \end{Bmatrix} \begin{Bmatrix} 1 & b & S \\ 1/2 & 1/2 & j' \end{Bmatrix} \\
&\times \begin{Bmatrix} l' & l & c \\ a & b & J \end{Bmatrix} \begin{Bmatrix} 1 & 1 & c \\ a & b & S \end{Bmatrix} \sum_{|m|=\Lambda} (-)^m \begin{pmatrix} 1 & 1 & c \\ -m & m & 0 \end{pmatrix}.
\end{aligned}
$$